International Journal of Earth Sciences (2020) 109:1377–1401
https://doi.org/10.1007/s00531-020-01846-4

ORIGINAL PAPER

Relationship between magnetic fabrics and deformation of the Miocene Pohorje intrusions and surrounding sediments (Eastern Alps)

László I. Fodor[1,2] · Emő Márton[3] · Marko Vrabec[4] · Balázs Koroknai[5] · Mirka Trajanova[6] · Mirijam Vrabec[4]

Received: 30 May 2019 / Accepted: 3 March 2020 / Published online: 30 March 2020

Abstract

The Miocene deformation history of magmatic and host metamorphic rocks and surrounding sediments was reconstructed by measuring meso- and microscale structures and anisotropy of magnetic susceptibility (AMS) data in order to constrain the structural evolution of the Pohorje pluton during the onset of lithospheric extension at the Eastern Alps–Pannonian Basin transition. Principal AMS axes, lineation and foliation are very similar to mesoscopic lineation and foliation data from the main intrusive body and from some dykes. Although contribution from syn-magmatic texture is possible, these structures were formed during the cooling of the pluton and associated subvolcanic dykes just shortly after the 18.64 Ma pluton intrusion. Dykes emplaced during progressively younger episodes reflect decreasing amount of ductile strain, while firstly mesoscopic foliation and lineation, and then the tectonic AMS signal gradually disappears. In the structurally highest N–S trending dacite dykes, the AMS fabric only reflects the magmatic flow. The Miocene sediments underwent the same, NE–SW to E–W extension as the magmatic and host metamorphic rocks as indicated by both AMS and fault-slip data. All these events occurred prior to ~ 15 Ma, i.e., during the main syn-rift extension of the Pannonian Basin and during the fastest exhumation of the Tauern and Rechnitz windows, both demonstrating considerable extension of diverse crustal segments of the Alpine nappe pile. After a counterclockwise rotation around ~ 15 Ma, the maximum stress axis changed to a SE–NW orientation, but it was only registered by brittle faulting. During this time, the overprinting of a syn-rift extensional AMS texture was not possible in the cooled or cemented magmatic, metamorphic and sedimentary rocks.

Keywords Anisotropy of magnetic susceptibility · Foliation · Lineation · Pluton · Dyke · Fault

Introduction

Numerous syn-magmatic structures, formed before complete crystallization, have been observed in granitic plutons (Bouchez 1997; Bouchez and Gleizes 1995; Talbot et al. 2004). Combined with solid-state structural elements, they provide important information about emplacement mechanism and regional structural evolution. While crystallization follows emplacement within a short time span, generally less than 1 Ma (Paterson et al. 1989), the age of the syn-magmatic and solid-state structures can be determined with good precision providing that the age of the intrusion and phases of cooling are determined by independent geochronological methods.

AMS is an excellent tool for studying small-scale deformation of different rock types (Graham 1954; Borradaile and Henry 1997). This method is particularly useful in granitoid intrusions and related dykes emplaced under varying

Electronic supplementary material The online version of this article (https://doi.org/10.1007/s00531-020-01846-4) contains supplementary material, which is available to authorized users.

✉ László I. Fodor
lasz.fodor@yahoo.com

1 MTA-ELTE Geological, Geophysical and Space Science Research Group at Eötvös University, Pázmány P. sétány 1/C, 1117 Budapest, Hungary

2 Department of Physical and Applied Geology, Eötvös University, Pázmány P. sétány 1/C, 1117 Budapest, Hungary

3 Paleomagnetic Laboratory, Mining and Geological Survey of Hungary, Columbus 13 u. 17-23, 1145 Budapest, Hungary

4 FNSE, Department of Geology, University of Ljubljana, Aškerčeva 12, 1000 Ljubljana, Slovenia

5 Geomega Ltd., Zsil u. 1, 1093 Budapest, Hungary

6 Geological Survey of Slovenia, Dimičeva ulica 14, 1000 Ljubljana, Slovenia

temperature and pressure. Specifically, AMS is frequently used to understand processes related to intrusions, such as syn-emplacement magmatic deformation or post-emplacement solid-state ductile structures (Djouadi et al. 1997; Kratinová et al. 2007; Stevenson et al. 2007). In addition, AMS can also be used to study metamorphic rocks (e.g., Hrouda and Janák 1976; Parés and van der Pluijm 2002; Ferré et al. 2003). In crystal-plastic shear zones, the AMS ellipsoid can reveal important information about the geometry of the foliation and the shear sense, and can be used to estimate shear strain (Borradaile 1991; Borradaile and Alford 1987; Till et al. 2010; and a review of Ferré et al. 2014). In intrusive and metamorphic rocks, the AMS axes can be compared to macroscopically observed foliations and lineations (e.g., Parés and van der Pluijm 2002; Hrouda and Janák 1976). The combined AMS and structural data can reveal a complex deformation history (Pomella et al. 2011; Georgiev et al. 2014). AMS can also reveal incipient deformation in sediments which seem to be undeformed in outcrop scale (Cifelli et al. 2004, 2009). In this case, the AMS axes are compared to strain or stress axes of the deformation observed in more intensely deformed, adjacent rocks (Borradaile and Jackson 2004).

Our study uses the techniques of AMS to determine the deformation history of the Miocene Pohorje pluton and adjacent metamorphic and sedimentary rocks in a region situated in the transition zone between the Eastern Alps and the Pannonian Basin. An important consequence of our study is that we were able to compare the AMS texture and structural elements within a variety of rock types and degree of anisotropy. The emplacement of the pluton was immediately followed by cooling and rapid exhumation to the surface which occurred within a time period of less than 3 Ma. This thermal evolution can be followed in the structures, i.e., deformation mechanism changed from crystal-plastic to brittle with the AMS fabric being formed within the former regime. The other aspect of our study reveals important information on the initiation of the Pannonian Basin system. The whole process from emplacement through cooling was coeval with the early phase of crustal thinning of the Alpine–Carpathian orogen, which led to the Pannonian Basin subsidence. Our results confirm dominantly extensional deformation which is recorded in both the AMS and plastic-to-brittle structures. This roughly E–W extension marked the syn-cooling deformation, and, together with early sediment deformation, reflects crustal stretching at the Alpine–Pannonian transition.

Geological setting

The Pohorje and Kozjak Mts. represent the easternmost outcrops of the Eastern Alps and the western marginal zone of the Miocene Pannonian Basin (Fig. 1). The deepest tectonic units in the massif belong to the Pohorje nappe (Janák et al. 2004) and are composed of metapelitic rocks (Hinterlechner-Ravnik 1971), diamond-bearing gneisses, which underwent UHP metamorphism in the Late Cretaceous (~95–92 Ma) (Janák et al. 2015; Sandmann et al. 2016). Metapelites incorporate lenses and bodies of marbles, quartzites, eclogites and garnet peridotites; the latter two lithologies also record UHP metamorphic conditions (Hinterlechner-Ravnik 1988; Miller et al. 2005; Vrabec et al. 2012).

The medium-grade metamorphic rocks are overlain by higher Upper Austroalpine tectonic units, which are built up of very low-grade Paleozoic and non-metamorphosed Permian–Triassic and late Cretaceous sediments (Mioč and Žnidarčič 1977) (Fig. 1). The major jump in metamorphic grade suggests that the original thrust contacts were overprinted during Late Cretaceous and Miocene extensional exhumation, the consequence of which is a mylonitic shear zone (Fig. 1, Fodor et al. 2002, 2008; Trajanova 2002).

The metamorphic rocks were intruded by the Pohorje pluton, an elongated magmatic body, about 30 km long and 4–8 km wide, with ESE–WNW orientation (Fig. 1) (Faninger 1970; Exner 1976; Mioč and Žnidarčič 1977). Original intrusive contact marked by thin metamorphic aureole was mapped along the margins (Mioč and Žnidarčič 1977; Žnidarčič and Mioč 1988). The pluton margin has been cut by N–S to NE–SW trending late faults.

The Pohorje pluton consists predominantly of granodiorite and tonalite (Dolar-Mantuani 1935; Faninger 1970; Zupančič 1994; Trajanova et al. 2008). Al-in hornblende barometry yielded pressure up to 7 kbar (Altherr et al. 1995) suggesting mid-crustal depth of about 20 km during intrusion. More recent data indicate a much shallower intrusion level for the NW than the SE end of the pluton, 3–4 and 6.2–7 kbar, respectively (Fodor et al. 2008, Sotelšek et al. 2019, Fig. 1). Aplite, pegmatite, "mafic" and dacite dykes occur both in the pluton itself and in the metamorphic country rocks (Kieslinger 1935; Mioč and Žnidarčič 1977), while the western part the pluton is transitional to subvolcanic dacite (Trajanova 2013). Since the surrounding Miocene sediments contain volcanoclastic levels (Winkler 1929; Mioč and Žnidarčič 1977), dacitic volcanic edifices, now completely eroded, must have also existed.

The age of the Pohorje pluton was uncertain for a long time. The intrusion was considered to belong to the Oligocene Periadriatic tonalite suite due to petrological and geochemical similarity and its geographical proximity to other Periadriatic intrusions (Mioč 1977; Pamić and Palinkaš 2000; Rosenberg 2004). New U–Pb IPCMS data on zircons, however, clearly demonstrate its late Early Miocene intrusion age (18.64 ± 0.11 Ma) (Fodor et al. 2008). This age has several implications for the magmatic and structural evolution of the Pohorje Mts. and wider area: (1) the pluton is very close in age to shallow subvolcanic and volcanic dacites

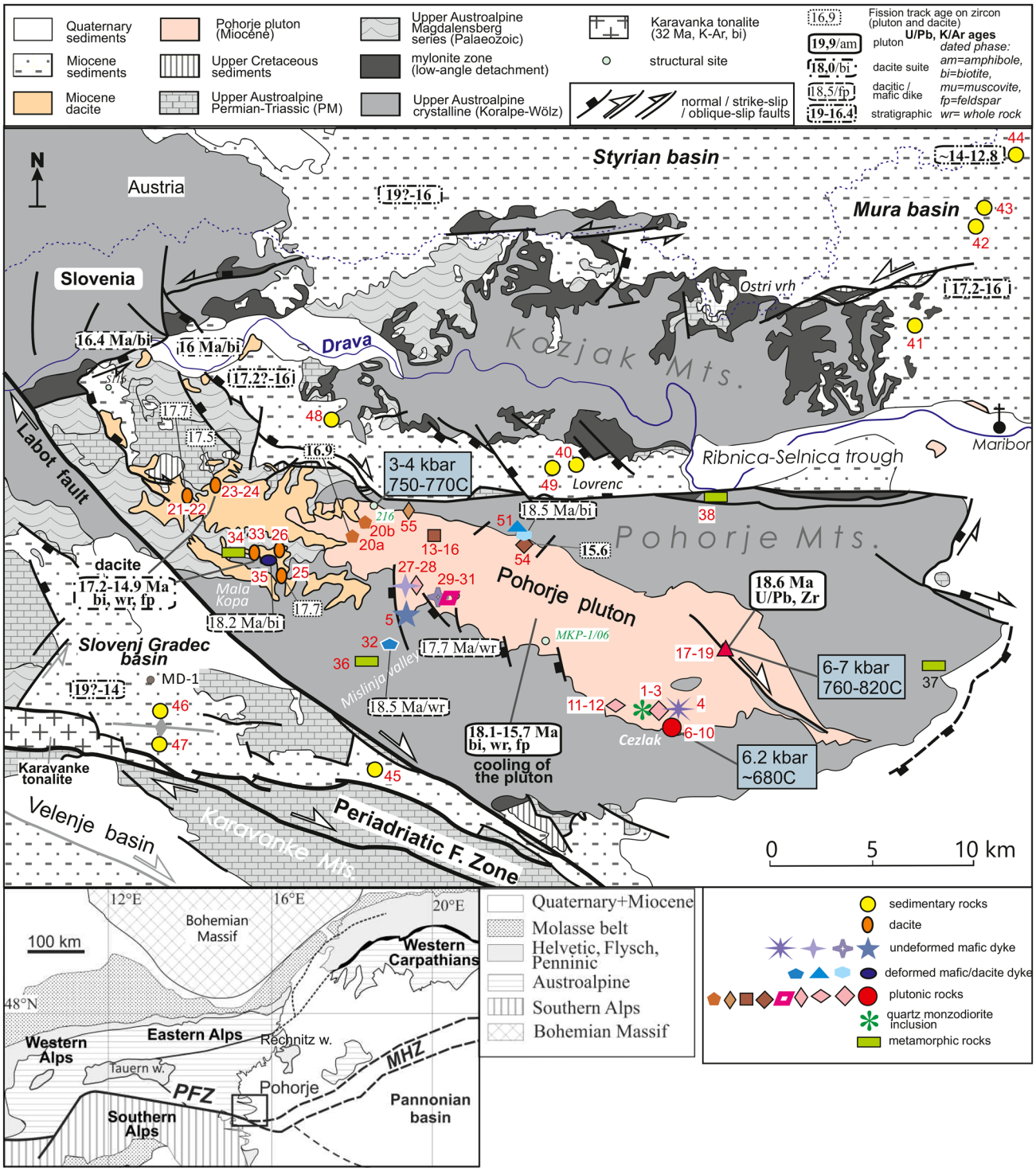

Fig. 1 Geological overview map of the study area with radiometric ages of various magmatic rocks in the Pohorje–Kozjak Mts., NE Slovenia (after Fodor et al. 2002, 2003, 2008; Trajanova et al. 2008, modified). Paleomagnetic sampling sites as well as pressure and temperature conditions determined previously for plutonic rocks are indicated. Inset shows location of the Pohorje–Kozjak area within the Alpine orogeny. MHZ: Mid-Hungarian Shear Zone

(17.7–14.9 Ma, Fig. 1). (2) The intrusion age is within 3 Ma of most of the K–Ar ages (18.1–15.7 Ma) from different minerals both from the pluton and subvolcanic dacitic rocks and also within 3 Ma of zircon fission track ages (Fig. 1.). These observations are interpreted as a sign of rapid uplift and related cooling from crystallization temperature below the partial annealing zone of zircon fission tracks (Fodor et al. 2008). (3) The intrusion overlaps in time with the initial magmatism of the Pannonian Basin (Harangi et al. 2005; Pécskay et al. 2006; Trajanova et al. 2008), and finally (4) the short time span from intrusion to rapid cooling also corresponds to the onset of lithospheric extension (rifting phase) of the Pannonian Basin system.

North of the Pohorje Mts., in the Ribnica–Selnica trough and on top of the Kozjak Mts., Miocene clastic sediments cover the older rock units (Fig. 1). They represent the marginal part of the Mura Basin, which is the westernmost sub-basin of the Pannonian Basin system. The late Early Miocene age of these sediments (Karpatian, 17.2–15.97 Ma, in Paratethys time frame; Sant et al. 2017) can also be projected from the main part of the Mura Basin, where a more than 1-km-thick deep marine succession was documented (Márton et al. 2002; Jelen and Rifelj 2003). Similar Miocene sediments also occur WSW of the Pohorje Mts. between the Labot and Periadriatic fault zones in the Slovenj Gradec basin (Fig. 1) which could also be part of the Mura Basin in a large sense, before the neotectonic uplift of the Pohorje Mts. and partial erosion of the covering once-continuous syn-rift sediments. Therefore, calcareous nannoplankton assemblage from the upper 860 m of the MD-1 borehole (Fig. 1) yielded NN4 and NN5 zones, representing Early to Middle Miocene (Karpatian to middle Badenian, ~ 17.2–14 Ma age, Ivančič et al. 2018). Below 860 m to a total depth of 1260 m, the section mostly represented slope sediments and was barren of calcareous nannofossils; hence, no biostratigraphic attribution was possible and an early Miocene age was proposed (Ivančič et al. 2018).

Methods

For most geological materials, magnetic susceptibility is an anisotropic property, which can be represented by a triaxial magnetic fabric ellipsoid with K_{max}, K_{int} and K_{min} axes. Their mean value is the bulk susceptibility of a rock sample. The magnetic susceptibility anisotropy (AMS) of a rock sample is controlled by paramagnetic (e.g., biotite, amphibole) and magnetic minerals (e.g., magnetite, hematite). When the bulk susceptibility is higher than a few times 10^{-4} SI, the contribution of the paramagnetic minerals to the susceptibility and to the AMS is considered negligible. The magnetic anisotropy of the magnetic minerals without the contribution of the paramagnetic constituents can also be calculated from the directional measurements of either the isothermal remanent magnetization (IRM) or of the anhysteretic remanent magnetization (ARM) imposed on the specimens in several directions in the laboratory.

The magnetic anisotropy measurements are carried out on samples fully oriented in situ in the field. At each sampling site, several samples were drilled, and the cores cut into standard-size specimens for laboratory analysis. The results of geographically closely related sites were sometimes evaluated together (this correspond to the widespread term "locality" in paleomagnetic terminology). The AMS of the specimens were measured in the Paleomagnetic Laboratory of the Mining and Geological Survey of Hungary using a KLY-2 Kappabridge. The statistical analysis of the AMS data was carried out on specimen level with a program developed by Bordás (1990) based on Jelínek (1977), on site level using the ANISOFT program (Hrouda et al. 1990; Chadima and Jelínek 2008; Chadima 2018; based on Jelínek 1978, 1981).

The rocks studied for magnetic anisotropy in the Pohorje area were mafic enclaves in granodiorites, typical granodiorites and dacites, mostly occurring as dykes. Additionally, we sampled dykes with variable but mostly andesitic composition; they were referred to as "lamprophyres" or "mafic dykes" in earlier works (Márton et al. 2006; Zupančič 1994). In addition, some samples represent quartz monzodiorite (locally called cizlakite) with very restricted occurrence limited to the SE part of the Pohorje pluton. We also investigated the late Early Miocene syn-rift sediments in the Ribnica–Selnica trough and in the Slovenj Gradec Basin, both structurally positioned at the margins of the Mura Basin. Additionally, we also sampled four sites in metamorphic rocks distributed around the Pohorje pluton.

Brittle structures were analyzed using fault-slip data. Stress inversion was performed with the software package of Angelier (1984). Phase separation was carried out by automatic (Angelier and Manoussis 1980) and manual methods. Special emphasis was put on the tilt test, in which a complete or partial backtilting of faults of a given phase was performed, using bedding as the reference horizon. When tilt test moved the symmetry plane of conjugate faults away from vertical, it was concluded that the faults were formed in their present-day position. If the symmetry plane of conjugate faults became vertical after backtilting, the faults were considered to have formed before the tilt event, and are therefore referred to as the pre-tilt faults.

In order to compare AMS and structural data, we made structural observations and took orientation measurements at the sites where paleomagnetic sampling for AMS was carried out. We also collected structural data at additional sites, mostly in the Miocene sediments, where paleomagnetic sampling was not possible (e.g., too coarse-grained clastics).

Results

Magnetic anisotropy measurements and results

In an earlier publication, Márton et al. (2006) pointed out that different rock types in the Pohorje Mts. exhibited a great variability in the magnetic susceptibility and in the degree of AMS (K_{max}/K_{min}), of the foliation (K_{int}/K_{min}) and lineation (K_{max}/K_{int}). Magnetic susceptibility data and values of degree of anisotropy, together with new data and with directional data of K_{max}, K_{int} and K_{min}, are now summarized in Fig. 2 and in Tables 1, 2 (see Supplementary material). The axial information is presented on maps and stereograms together with macroscopic structural data (Figs. 4, 6) and will be discussed successively.

Weak susceptibility, low degree of AMS and somewhat scattered principal susceptibility directions characterize the quartz monzodiorite, suggesting a very weak internal deformation. From the granodiorite outcrops, mainly mafic enclaves (2–4 large ones from one outcrop) were drilled, which contained more mafic minerals than the host rock itself, and were usually finer grained and less hard for drilling. Both the host rock and the enclaves have typically high susceptibilities, (in the range of 10^{-3}–10^{-2} SI) high to extremely high degree of AMS anisotropy (Fig. 2) and fairly well-defined magnetic fabric, both on site (e.g., within individual enclaves) and locality (a quarry) level. The grouping of the principal susceptibility directions is good on both site and locality level. According to the orientation of the magnetic foliation planes and the directions of the magnetic lineations, several groups can be distinguished which will be described later (e.g., Fig. 4).

Among the "mafic" (andesitic) dykes, the susceptibilities of two sites (27 and 29 in Fig. 2) are much higher (10^{-2}–10^{-1} SI), matching those of the granodiorite enclaves with the highest susceptibilities, but the degree of AMS anisotropy is moderate (around 1.15). Six other dykes are characterized by susceptibilities in the 10^{-4}–10^{-3} SI range, i.e., similar to the monzodiorite and the degree of AMS anisotropy is between 1.05 and 1.18 (sites 4, 5, 32, 51b, c, 54).

Some sampled dykes form a distinct group, which shows a variable but observable sign of mesoscopic and microscopic deformation, mostly foliation. They will be referred to as "deformed dykes" in the following. Sites 35 and 51a of dacitic and andesitic composition are the most striking, where the extremely large degree of anisotropy associated with well-grouped anisotropy axes clearly reflects the mesoscopic deformation. Site 54 bears somewhat larger anisotropy than other dykes of this susceptibility range, and an incipient foliation is present. The difference in anisotropy is the smallest between spatially closely related dykes 32 and 5. The mesoscopic deformation is also the smallest in site 32 where only dyke margins show a foliation.

The magnetic susceptibilities of the dacites are in the 10^{-2} SI range, and the degree of the AMS anisotropy is typically below 1.05. The orientations of the AMS fabrics show some variations between localities, but the best developed fabrics exhibit lineations close to the N–S direction.

Among the metamorphic rocks, those of site 34, which consist of low-grade Paleozoic slate contact metamorphosed by a young dacite dyke (Fig. 1), showed a low degree of

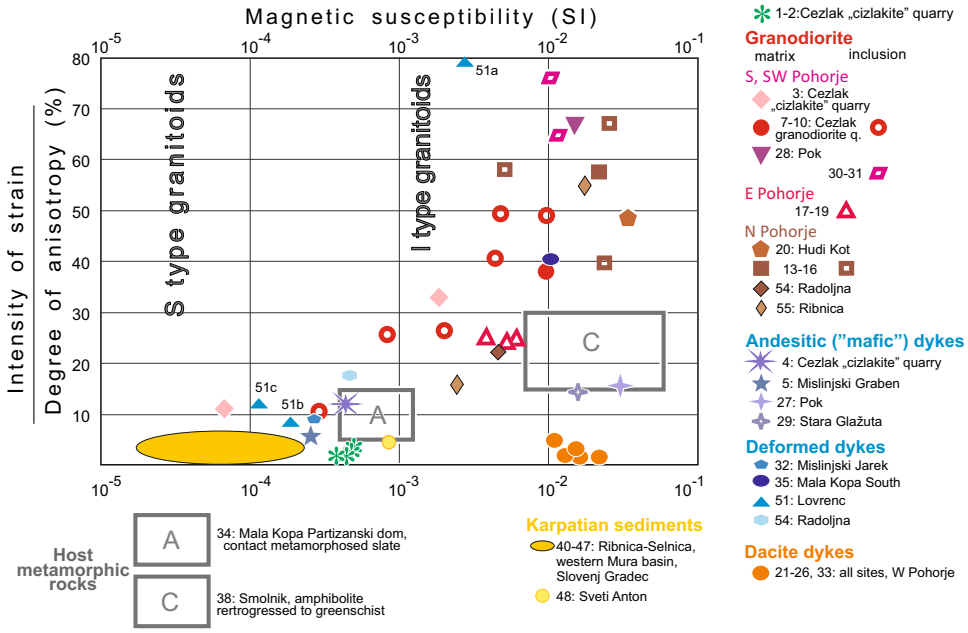

Fig. 2 Anisotropy data in function of degree of anisotropy for the Pohorje intrusions (including dykes), syn-rift sediments and host metamorphic rocks

AMS, with susceptibility in the range of 10^{-3} SI. Amphibolites were studied from three localities. They exhibit similarly large susceptibility values but lower anisotropy as the Miocene plutonic rocks (Fig. 2, sites C).

All sediments exhibit susceptibility in the 10^{-4}–10^{-5} SI range, except for site 48 (~ 10^{-3} SI), and the anisotropy is very low, below 1.1 (Fig. 2). All sites show good clustering of AMS axes, and all but one site were tilted after the acquisition of the magnetic texture; tilt test clearly shows that AMS fabric predates the tilting (or fault-related folding).

Structural data

Deformation in plutonic rocks

The predominantly granodioritic rocks of the Pohorje pluton in most cases show an oriented fabric, i.e., a foliation and locally they also show an associated mineral lineation (Fig. 3a). Intensity and frequency of these structural elements vary with sampling sites and lithology, and depend on the origin of foliation. In general, the foliation is less developed in the plutonic rocks than in the host metamorphics.

The orientation of biotite and amphibole grains was considered to be of magmatic in origin, if no (or negligible) signs of subsequent solid-state deformation could be observed in the rock. Clear evidence for solid-state deformation is ubiquitous and totally overprints the preexisting magmatic fabric, when the former is well-developed.

On a microscale, the solid-state deformation in the plutonic rocks is best marked by the advanced, frequently complete, dynamic recrystallization of quartz by "fast" grain-boundary migration (GBM; Stipp et al. 2002) indicated by the grain-boundary morphology within the recrystallized aggregates (Fig. 3b). The deformed quartz grains are arranged into elongated lenses and ribbons in the most heavily deformed samples (Fig. 3c, e). In less deformed rocks, quartz is only partly recrystallized, and relict grains show intensive undulose extinction and the formation of subgrains. Along the northern pluton margin quartz recrystallization also occurred by subgrain rotation (Fig. 3c).

Primary biotite was locally sheared and partly recrystallized into highly elongated, fine-grained tails along the foliation. Feldspars show basically brittle behavior as evidenced by intra- and intergranular fractures crosscutting well-preserved magmatic zonation and twins. However, the presence of tapering deformation twins, bent twins, the occurrence of myrmekites at stressed grain contacts, and the variably developed core–mantle structures indicate that limited crystal-plastic deformation also occurred at several locations.

All these microstructural features indicate deformation temperatures characteristic of medium-to-high-temperature greenschist facies, in agreement with earlier results of Fodor et al. (2008). Varying deformation features could form during the cooling path within the greenschist field.

In the SE part of the pluton, the small quartz monzodiorite body shows a contrasting deformation. The foliation in the granodiorite is well-developed close to, and wraps around the rigid, angular monzodiorite boudins (Fig. 3f), while away from blocks, the foliation is less intensive. At the contact of the two lithologies, shear zones occur with chloritic lineation. S–C foliation observed both at meso- and microscale indicates oblique dextral-normal top-to-ENE shear (Fig. 3e, f). In contrast, the quartz monzodiorite does not show any mesoscopic ductile deformation. On a microscale, undulose extinction of secondary amphibole, quartz and K-feldspar can be seen, and plagioclase can exhibit deformational twins.

Original mapping data (Mioč and Žnidarčič 1977; Fodor et al. 2008) and new field observations suggest that the pluton has different dip domains with variable foliation orientation. At the northern pluton margin, foliation is clearly formed by solid-state shearing and is sub-parallel to foliation in surrounding host metamorphic rocks. Both rock suites are moderately to steeply south dipping; therefore, the plutonic rocks are here structurally above metamorphic rocks (Fig. 4b). The moderately or poorly developed lineation is gently east–southeast or west–northwest plunging, except for a steep oblique lineation near the NW pluton margin (site S216, Fig. 4a). In the internal part of the pluton, foliation strike makes a small angle to the pluton margin (Fig. 4b, sites 13–16). At the western pluton termination, the foliation orientations vary considerably (Fig. 4a, sites 20a, b). Therefore, the foliation is mainly defined by oriented biotites, and could be partly magmatic in origin.

Foliation becomes gently SW dipping in the eastern part of the pluton (near sites 17–19, Fig. 4b), where the host metamorphic rocks dip below the pluton. Slightly westward, north of Cezlak, the plutonic rocks are covered by a cap of metamorphic rocks (Fig. 4b). Everywhere south and south westward of this cap, the map-scale geometry of the intrusion contact clearly shows that the pluton dip southward under the metamorphic host rocks. This geometry is entirely in agreement with the conclusion of Kirst et al. (2010) that the southeastern tail of the pluton exhibits both its upper and lower contacts, implying its gently southwest dipping position, as well as its relatively small thickness. In the eastern pluton, the lineation strike is close to N–S (Fig. 4a).

Along the southern margin of the pluton, the foliation dips gently to the SE or WSW, making a small angle to the south dipping pluton boundary which slightly undulates due to intersections with the topography (Fig. 4). The lineation gently plunges E or W, being oblique or downdip within the foliation planes (Fig. 4). The scatter in the orientation

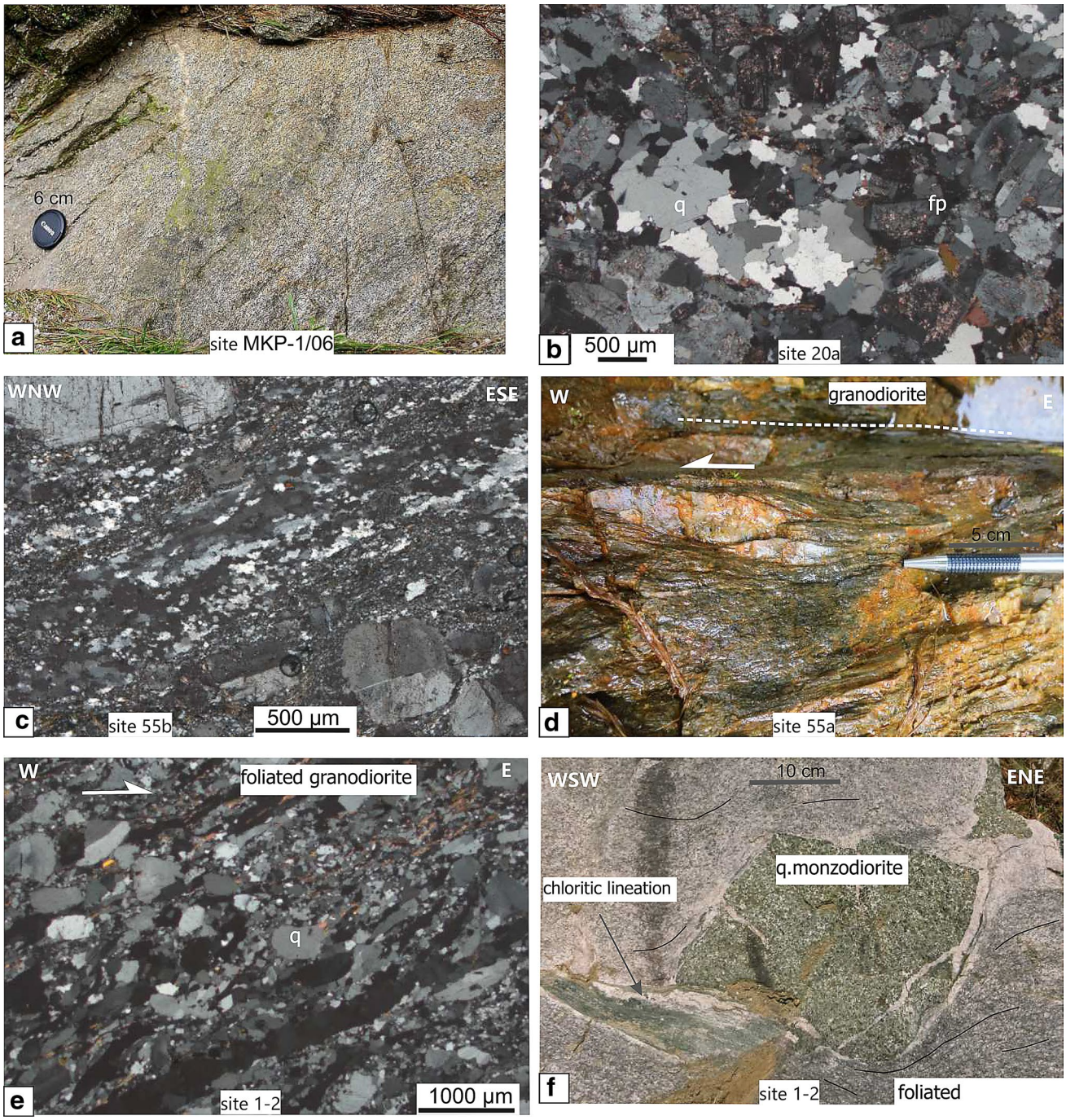

Fig. 3 Deformation features in the granodiorite pluton, and in the Cezlak quartz monzodiorite body. **a** Field example of foliation in the granodiorite. **b** Dynamically recrystallized quartz and internally undeformed, zoned feldspars in granodiorite. Quartz fabrics indicate grain-boundary migration (GBM) as recrystallization mechanism, in northwestern pluton. **c** Quartz aggregates recrystallized by sub-grain rotation along the northern pluton margin. **d** Map view picture just at the northern contact of the granodiorite, in host metamorphics. Quartz lens indicates sinistral shear sense. **e** Microfabrics of a moderately northeast-dipping shear zone at the contact of quartz monzodiorite and granodiorite. Moderately developed S–C foliation indicates top-to-E (oblique extension) shear sense. **f** Map view of foliated granodiorite wrapping internally undeformed quartz monzodiorite. A larger body was sampled for AMS study. Locations of sites see Fig. 1

of the foliations is at least partly due to later deformation, but could locally also represent primary magmatic foliation geometry. In this part of the pluton, sub-vertical shortening is also indicated by strongly flattened mafic xenoliths and weakly foliated aplite–pegmatite dykes (Fodor et al. 2008). We classify all these deformation features as D1 structures, despite their variable geometry.

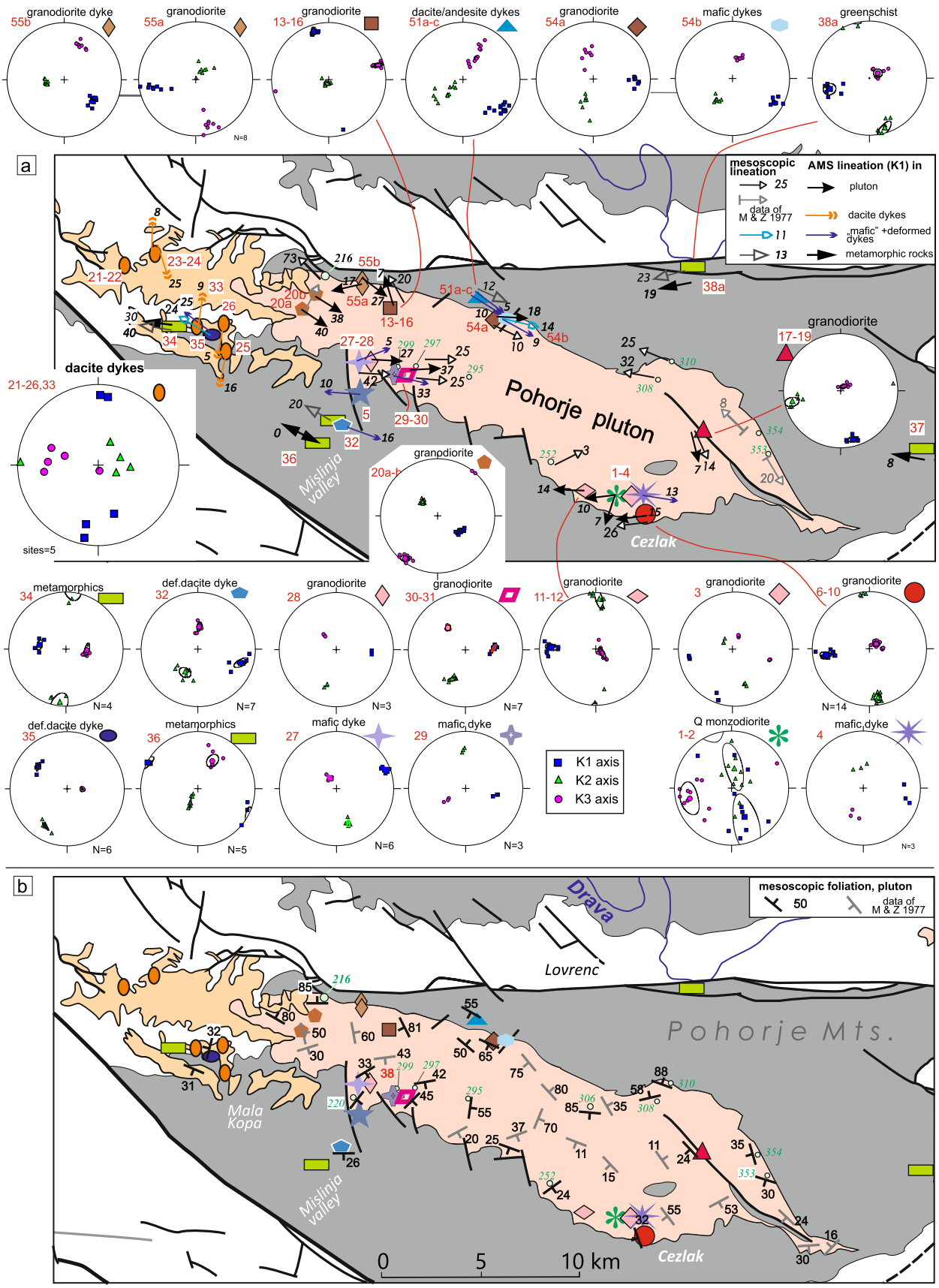
granodiorite dyke
55b
granodiorite
55a
granodiorite
13-16
dacite/andesite dykes
51a-c
granodiorite
54a
mafic dykes
54b
greenschist
38a
a
mesoscopic lineation
AMS lineation (K1) in
25
pluton
data of M & Z 1977
dacite dykes
„mafic" +deformed dykes
11
13
metamorphic rocks
Pohorje pluton
dacite dykes
21-26,33
sites=5
granodiorite
17-19
granodiorite
20a-h
Mislinja valley
Cezlak
metamorphics
34
N=4
def.dacite dyke
32
N=7
granodiorite
28
N=3
granodiorite
30-31
N=7
granodiorite
11-12
granodiorite
3
granodiorite
6-10
N=14
def.dacite dyke
35
N=6
metamorphics
36
N=5
mafic dyke
27
N=6
mafic dyke
29
N=3
K1 axis
K2 axis
K3 axis
Q monzodiorite
1-2
mafic dyke
4
N=3
b
mesoscopic foliation, pluton
50
data of M & Z 1977
Drava
Lovrenc
Pohorje Mts.
Mala Kopa
Mislinja valley
Cezlak
0
5
10 km

◂**Fig. 4** Structural and AMS data in the Pohorje–Kozjak area. **a** Map of AMS and mesoscopic lineations, together with AMS stereoplot data; **b** map of mesoscopic foliation. Symbols for sites are the same as in Figs. 2 and 6 and appear both on the maps and at upper right-hand corner of stereograms. Red and green labels indicate sites for AMS and structural studies. Lithological and structural symbols as in Fig. 1. Stereograms are on lower hemisphere projection, their legend is in Fig. 9. M & Z: data of Mioč and Znidarčić (1977)

Dykes and their deformation

The pluton and its surroundings are cut by 1–10-m-thick subvolcanic dykes having the composition of andesite with varying contents of biotite and amphibole. Dacite dykes occur in the host metamorphics. The former group was called "mafic dykes" in the paleomagnetic studies of Márton et al. (2004, 2006). Phenocrysts within fine-grained matrix indicate that the intrusion depth of the dykes was less than that of the main granodiorite body.

The most dominant outcrop-scale ductile structure is the weakly to moderately developed foliation sub-parallel to the dyke–host rock contact, and its intensity generally changes within a single dyke (Fig. 5a, b). In closely spaced dacite dykes of site 51a-c (Fig. 4a), the foliation drastically changes from one dyke to another, although spatially they are only 10 m apart. Near the main dacite body, in one dyke (site 35, Fig. 4a), the foliation is well-developed and contains a WNW plunging stretching lineation. Dykes in the north (sites 51, 54, Fig. 4a) exhibit poorly developed mineral lineation. In site 54, the intensity of the foliation is stronger in the granodiorite than in the intruding dykes; thus, the onset of crystal-plastic deformation in the pluton preceded the dyke emplacement.

On a microscale, the original magmatic quartz has been internally deformed into elongated lenses, locally up to ribbon quartz (Fig. 5). Relic grains display undulose extinction and subgrains, whereas new grains with serrated grain boundaries were formed by dynamic recrystallization. Biotite and amphibole grains are often sheared, and suffered pressure solution along foliation planes. Amphiboles are twinned along their long axis. Part of the feldspars phenocrysts is idiomorphic with magmatic zoning and shows brittle fracturing (Fig. 5a–c). Some large feldspar phenocrysts show undulose extinction and subgrain formation, and locally they display core and mantle structures (Fig. 5b). The shape-preferred orientation of quartz grains in dynamically recrystallized quartz aggregates feldspar sigma clasts, mica and amphibole fishes, (sites 51, 54; Fig. 5a–d), and weakly developed shear bands indicate a consistent shear sense; it is top-to-WNW (extensional) in the western site 35 (Figs. 4a, 5b) and top-to-ESE (normal-sinistral) in the northern dykes (Fig. 4a).

Dynamically recrystallized quartz, boudinaged biotite and deformation features in feldspars broadly place the deformation into the higher greenschist facies. Variably deformed feldspars indicate progressively lower temperature for deformation initiation. This can be a sign of deformation during cooling, just after dyke emplacement when dyke temperature was still high enough to enhance its crystal-plastic deformation.

Sub-vertical andesite dykes within the southern part of the pluton do not show any mesoscopic ductile deformation, but in thin section display aligned biotite and amphibole, which can be attributed to magmatic flow (Fig. 5f, sites 27, 29, 4). Evidence for crystal-plastic deformation is generally lacking, except for minor subgrain formation in some quartz phenocrysts (site 29).

The westerly located sub-vertical or steeply dipping dacite dykes clearly crosscut the foliation of the host metamorphic rocks (Fig. 5g). In such dykes, only brittle deformation is detected in the form of tensional joints and small faults; these structures generally show symmetry planes parallel to dyke margins. In thin section, oriented biotite, amphibole or feldspar can locally be observed, and this texture is attributed to magmatic flow (Fig. 5h).

Brittle deformation in syn-rift sediments and magmatic rocks

Karpatian sediments north of the Pohorje Mts. exhibit a great number of small-displacement brittle faults, which belong to several deformation events. The majority of faults have normal or normal–oblique kinematics, while others are strike-slip faults; reverse faults are rare. Displacements for normal faults vary from cm to few meters, but the maps clearly indicate larger displacement in the order of 100–1000 m. Faulting resulted in tilted blocks, in which bedding dip can reach 30° to 40°. Near the normal faults, the beds show folding; the combined effect of drag and tilt in opposite directions resulted in fault-related folds.

Paleostress calculations indicate two main directions of σ_3 axis. One group of sites incorporates faults with tension oriented between NNE–SSW and E–W, while the other one has σ_3 axes E–W to SE–NW directed (Fig. 6a, b). The strike of outcrop-scale normal faults changes correspondingly from NW–SE to NE–SW. Oblique slip is also frequent, both at map- and outcrop scale. All these faults are classified into the D1(b) (b = brittle) and D2 deformation phases. We also attributed brittle faults observed in the plutonic and metamorphic rocks to these deformation phases D1(b) to D2. They clearly postdate crystal-plastic structures and were formed after the cooling of the rocks.

Consistent relative chronology exists between these phases; faults of D1(b) mostly predate the tilting, while D2 fractures everywhere formed after the tilting. The

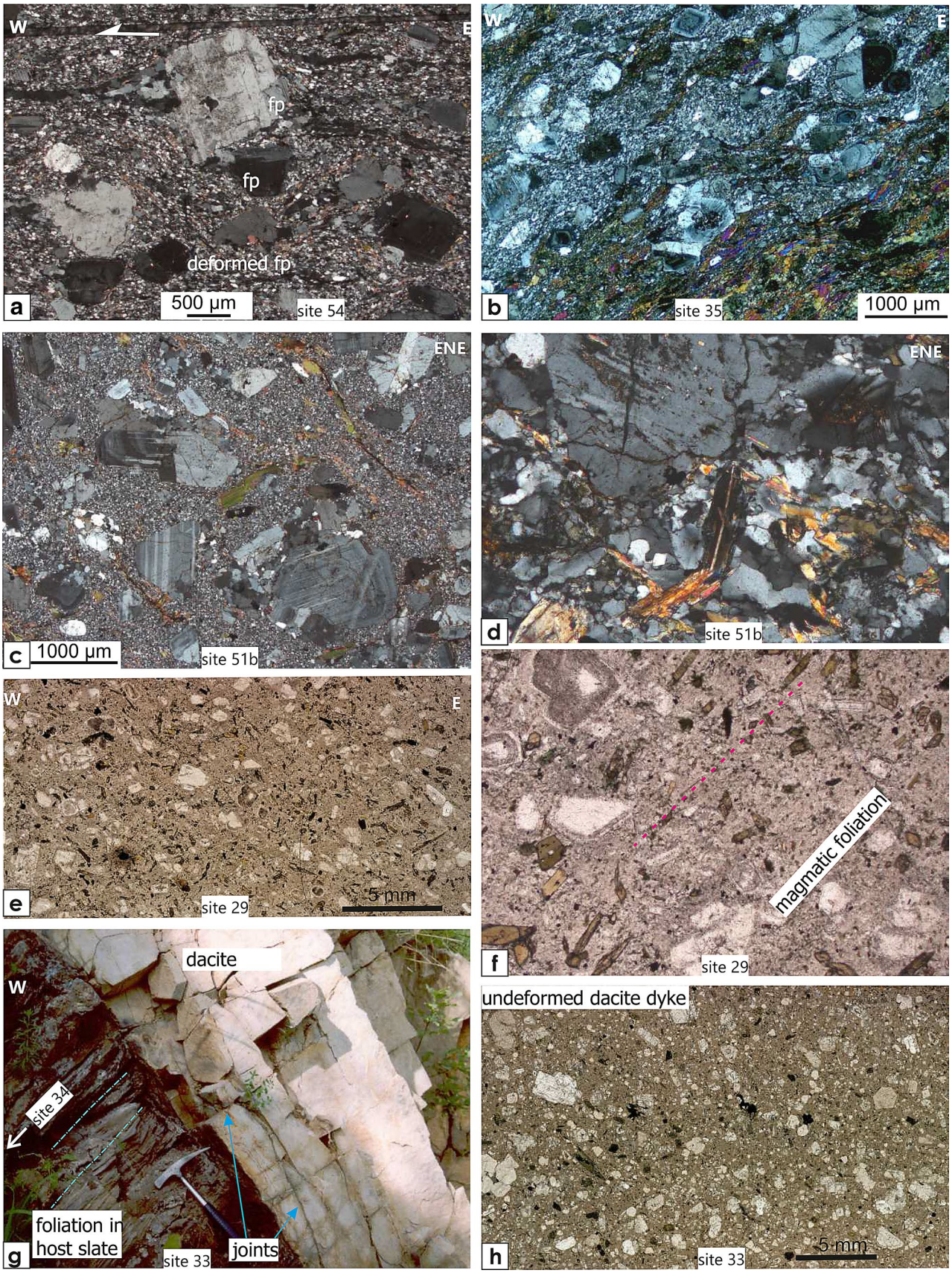
W
E
fp
fp
deformed fp
500 µm
a
site 54
W
E
b
site 35
1000 µm
ENE
c
1000 µm
site 51b
ENE
d
site 51b
W
E
e
site 29
5 mm
magmatic foliation
f
site 29
dacite
W
site 34
foliation in
host slate
g
site 33
joints
undeformed dacite dyke
h
site 33
5 mm

◂**Fig. 5** Deformation features in variably deformed dacite and andesite dykes. **a** Sigma clasts in foliated andesite dyke, at the northern margin of the pluton, within granodiorite, sub-horizontal view. Note recrystallized quartz grains and zoned undeformed feldspar grains. **b** Strongly foliated dacite dyke, and its contact with host micaschist, in the western dacite body. **c** Weakly oriented texture in a dacite dyke intruding metamorphic rocks, just near the northern contact of the granodiorite. Section perpendicular to dyke margin. **d** Dynamic recrystallization of primary feldspar phenocrysts at the margin of the same dacite dyke as in **c**, 20 cm away. **e** Scanned picture of a thin section of an N–S trending "mafic" (andesite) dyke, in the southern pluton. Note weakly developed magmatic foliation. **f** Thin section from the same dyke with oriented biotite, amphibole crystals. **g** Field view of undeformed dacite dyke intruded in foliated Paleozoic slate. Note joints parallel to dacite dyke wall and also to host rock foliation. **h** Scanned view of thin section from the same dyke as in **g**. Locations of sites, see Fig. 1

reactivation of dip-slip faults by oblique slip also suggests a clockwise change in tensional direction from D1 to D2 phases (e.g., site S-353, Fig. 6b).

Conjugate strike-slip faults also occur at several sites and indicate a broadly N–S to NNE–SSW compression, and perpendicular tension. Their relative chronology with respect to tilting and normal faults is not unequivocal; in most cases, they were formed after the tilting, but exceptions also exist and some could have formed, while the beds were still horizontal, i.e., before normal faulting and the associated tilting (e.g., S67, S116, Fig. 6a). Pre-tilt strike-slip faults could represent spatial variation of the deformation style within the dominantly extensional syn-rift phase, and we include them within the D1(b) phase (Fig. 6a). Fodor et al. (2008) argued that post-tilt strike-slip faults represent a separate (neotectonic) phase that could be latest Miocene to Quaternary in age (annotated as D3 in Fig. 6b).

Comparison of AMS fabric and mesoscale structures

In this section, we compare principal AMS axes and mesoscale structural features, namely foliation/lineation data from magmatic rocks and the strike of the dykes. We also took into account fault-slip data which complete the deformation history although in magmatic rocks brittle deformation postdates the temperature range during which the AMS fabric could develop. The brittle structures are the only mesoscale deformation features within the Miocene syn-rift sediments, which can be compared with AMS data.

Comparison of data from plutonic rocks

In the southern part of the Pohorje pluton, the magnetic foliation is gently dipping, which is reflected by steep K_3 axis coinciding with mesoscopic foliation poles (Fig. 7c). The degree of AMS is very high (Fig. 2), atypical for undeformed granitic pluton, suggesting that the granodiorite acquired the magnetic fabric under the influence of tectonic stress. Mineral and magnetic lineations (K_1 axis) are E- or W plunging and closely match each other (Figs. 4a, 7c).

The quartz monzodiorite blocks (sites 1–3) show peculiar AMS data and need a detailed description. In the monzodiorite boudins, the degree of the AMS anisotropy is low (Fig. 2), and only the K_{min} axis is well-defined. This axis is parallel to σ_1 axis calculated from a few oblique striations occurring on brittle fault planes (Fig. 7a). We consider these features to be coincident, although the two methods may describe two deformation episodes with different mechanisms. As we described earlier, the granodiorite surrounding the monzodiorite boudins exhibits bent foliation and chloritic lineations (Fig. 3e, f), which, although occurring on variably oriented planes, are kinematically and geometrically coherent, and indicate an ENE–WSW elongation (Fig. 7b). However, a few lineations are consistent with a NNE–SSW extension direction. The variation is probably due to the complex geometry of the shear zones around the quartz monzodiorite boudins. This double orientation pattern is reflected in the AMS data (Fig. 7b), in which the two groups in K_{min} axes orientation are parallel to the suggested extensional directions.

The contrasting AMS texture and deformation geometry is the expression of different deformation mechanisms; while the granodiorite shows signs of crystal-plastic deformation at greenschist facies deformation, the monzodiorite mostly remained internally undeformed (Fig. 3f). These observations support the interpretation that monzodioritic blocks might have been incorporated into the granodioritic melt, and their magnetic fabric may refer to an earlier episode and remained unaffected by subsequent solid-sate deformation of the granodiorite. The contrasting strain between the two rock types is visible in their deformation pattern and in their AMS characteristics, both in degree of deformation and the orientation of the principal axes.

Some of the data in the eastern part of the pluton show good coincidence of AMS and structural data from ductile fabric (Figs. 4, 7d). Along the northern pluton margin most magnetic fabric is parallel to the well-developed, moderately to steeply dipping foliation and gently plunging lineation of the granodiorite as well as to the strike of the pluton boundary (Figs. 4a, b, 7e). Within these sites (55a, 54, Fig. 7e), foliation is locally E–W trending and thus making a small angle to the generally WNW trending foliation. We attribute this angular difference to specific locations within the shear zones along the pluton–host rock contact. Similar angular differences are typical for shear zones, where the AMS ellipsoid is between the S and C foliation planes (Sidman et al. 2015; Zhou et al. 2002). Finally, in few sites, the magnetic fabric and mesoscale structures slightly deviate in orientation from this general WNW–ESE trend toward NNW trend (e.g., sites 13–16, Fig. 7f).

In the westernmost part of the pluton, the AMS and structural data do not fit well (sites 20a & b, Figs. 4, 7g). Mesoscale foliation is sub-vertical and N–S trending, whereas two of the AMS axes are inclined, and all AMS axes are oblique to structural foliation planes. We cannot explain this discrepancy yet. Apart from this problematic area, we generally find that the magnetic fabric reflects the deformation pattern. In most cases, the deformation occurred in solid state, although sometimes it could follow precursor

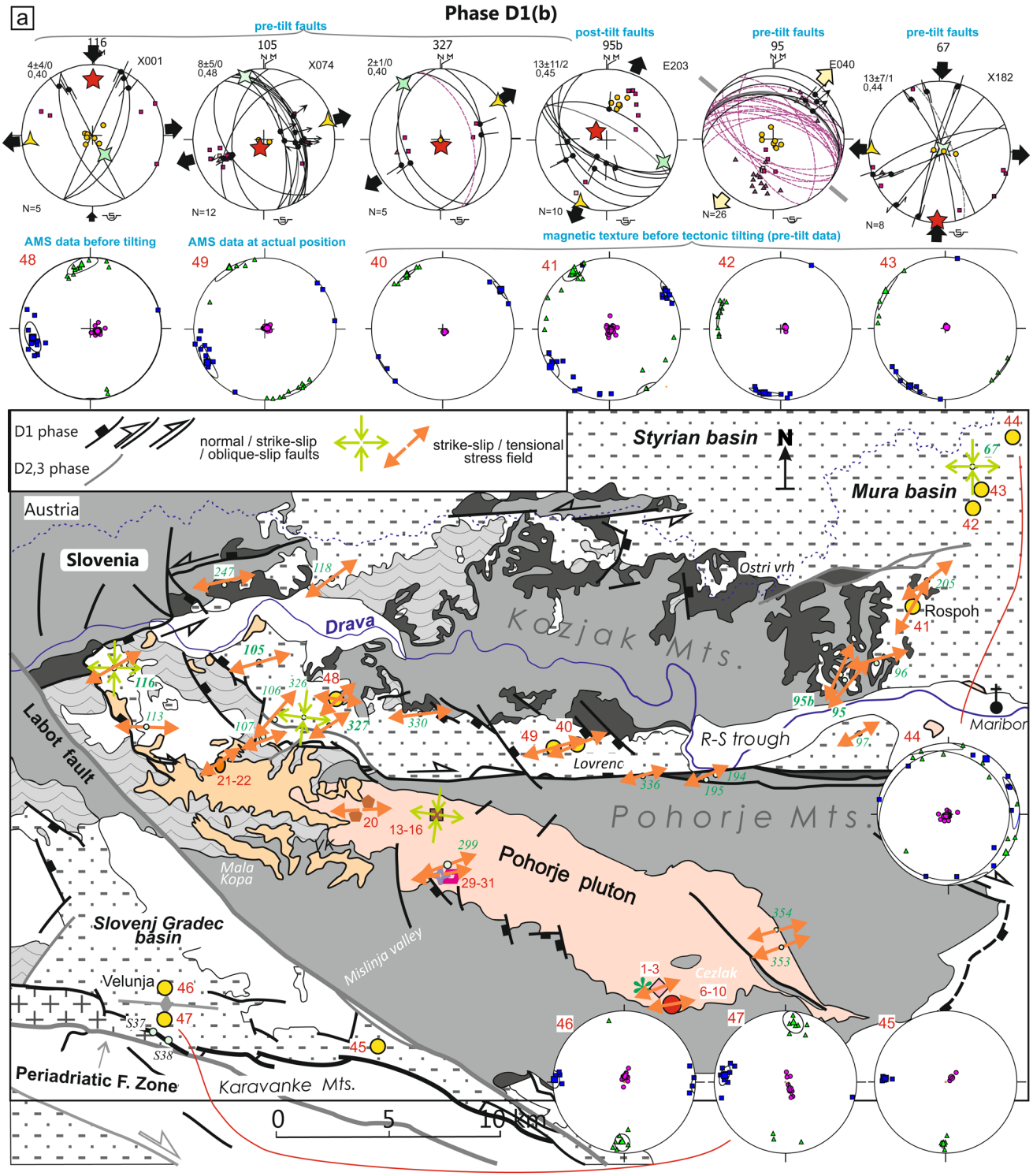

Fig. 6 Map of AMS Kmax axes, stress axes and AMS stereoplots from syn–rift sediments. Lithological and structural symbols as in Fig. 1. Stereograms are on lower hemisphere projection, their legend is in Fig. 9

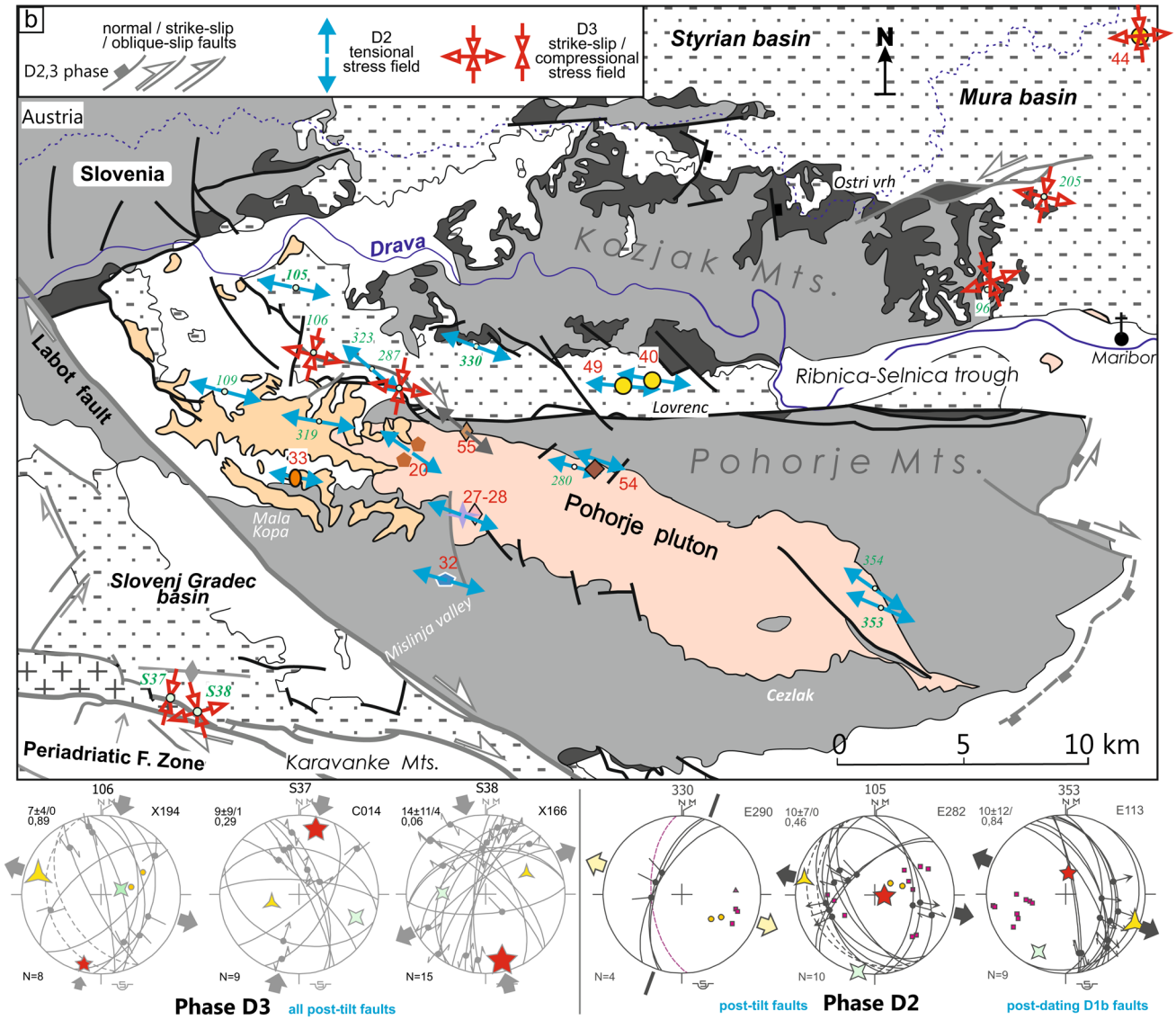

Fig. 6 (continued)

magmatic foliation marked by the alignment of biotite and amphibole.

In the southern part of the pluton, post-cooling D1(b) brittle structures still record ~ E–W directed extensional strain similar to that recorded in the crystal-plastic fabric, whereas at the northern margin, both the AMS and the younger D1(b) brittle fractures seem to be compatible with strike-slip deformation, exhibiting roughly the same ~ E–W extension direction (Fig. 7c, e, respectively). However, in the eastern part of the pluton, the AMS fabric is slightly deviating from D1 phase and the younger fractures appear to belong to a different deformation event, the D2 phase.

Comparison of data from dykes

Mesoscopically undeformed dacite dykes show well-defined AMS fabrics regardless of their location either north (sites 21–24) or south (sites 25, 26, 33) of the main dacite body (Fig. 8a). The K_{max} axes are typically N–S oriented, while minimum axes are mostly sub-horizontal. The strike of the dykes matches perfectly the orientation of near-horizontal maximum AMS axes. However, no internal deformation of the rocks is visible in thin sections (Fig. 5f) which suggests that the AMS fabric is coeval with magma emplacement. Parallelism of K_{max} and the dyke strike suggests that the AMS reflects magmatic flow which occurred parallel to the dykes (Tarling and Hrouda 1993; Chadima 2018). The formation of dykes is associated with extensional stress; therefore,

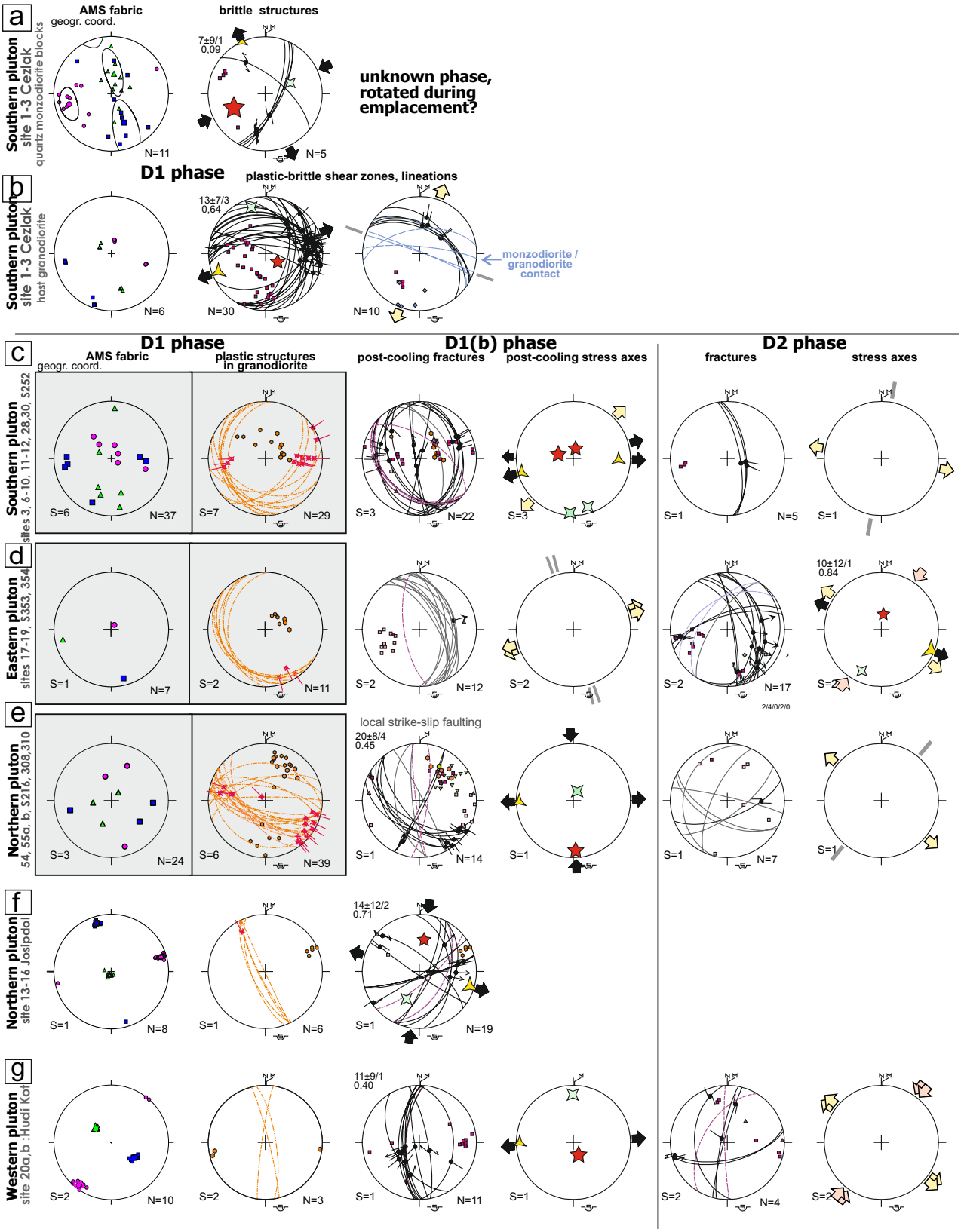
a
AMS fabric
geogr. coord.
brittle structures
Southern pluton
site 1-3 Cezlak
quartz monzodiorite blocks
7±9/1
0,09
N=11
N=5
unknown phase,
rotated during
emplacement?
D1 phase
plastic-brittle shear zones, lineations
b
Southern pluton
site 1-3 Cezlak
host granodiorite
13±7/3
0,64
N=6
N=30
N=10
monzodiorite /
granodiorite
contact
D1 phase
D1(b) phase
D2 phase
c
AMS fabric
geogr. coord.
plastic structures
in granodiorite
post-cooling fractures
post-cooling stress axes
fractures
stress axes
Southern pluton
sites 3, 6-10, 11-12, 28,30, S252
S=6
N=37
S=7
N=29
S=3
N=22
S=3
S=1
N=5
S=1
d
Eastern pluton
sites 17-19, S353, 354
S=1
N=7
S=2
N=11
S=2
N=12
S=2
S=2
N=17
2/4/0/2/0
10±12/1
0.84
S=2
e
Northern pluton
54, 55a, b, S216, 308,310
local strike-slip faulting
S=3
N=24
S=6
N=39
20±8/4
0.45
S=1
N=14
S=1
S=1
N=7
S=1
f
Northern pluton
site 13-16 Josipdol
S=1
N=8
S=1
N=6
14±12/2
0.71
S=1
N=19
g
Western pluton
site 20a,b :Hudi Kol
S=2
N=10
S=2
N=3
11±9/1
0.40
S=1
N=11
S=1
S=2
N=4
S=2

◂**Fig. 7** Comparison of AMS and outcrop-scale structural data from the pluton, including the quartz monzodiorite of Cezlak. D1(b) fractures are younger than the AMS fabric, but considered as part of the same D1 phase. Gray boxes indicate averaged AMS and structural data. Fractures, stress axes are measured, calculated or estimated from individual sites, but shown together. Geogr. coord.: data in geographic coordinate system (actual position). Tectonic coord. system contains data backtilted to horizontal bed position. Gray frame marks compared data sets, dashed when uncertain. S at lower left corner marks the number of sites. The number of data involved is at lower right-hand corner. Upper left corner: average misfit angle, calculated for all faults with standard deviation, with respect to the ideal stress axes/number of misfit data; lower line: ratio $\varphi = \sigma_2 - \sigma_3/\sigma_1 - \sigma_2$

the N–S orientation of the dyke margins suggests an E–W minimum stress axis (Fig. 8a). It is noted that post-cooling brittle fractures also indicate the E–W extension (Fig. 8a). However, tectonic stresses are only indirectly responsible for AMS fabric, and they simply controlled dyke geometry and hence magmatic flow.

The andesitic ("mafic") dykes intruded into the southwestern Pohorje Mts. show a complex deformation history. The AMS fabric in the dykes of the sites 4, 27 and 29 shows ~ E–W maximum axis which is perpendicular to the strike of the dykes (Figs. 4a, 8b). This AMS fabric may reflect the continuation of extensional deformation which opened the dykes and subsequently affected the magnetic fabric of the crystallizing dyke. Deformation is also suggested by the degree of anisotropy, which is much higher here than at "typical" dacite localities in the west (21–26, 33, Fig. 2). The microstructure of the mafic dyke rocks does not show strong crystal-plastic deformation (Fig. 5e, f), and their weakly oriented texture is probably mostly magmatic in origin, connected to viscous deformation in the final stage of crystallization (sensu Mancktelow and Pennacchioni 2013). Post-cooling faulting still shows similar E–W directed extensional stress [Fig. 8b, phase D1(b)]; this may suggest that deformation was closely coaxial from dyke emplacement, subsequent week crystal-plastic deformation to brittle faulting during cooling. It was followed by a clockwise change in extension direction during D2 phase.

SW and W from the Pohorje pluton, two deformed dacite dykes containing mafic minerals are intruded along the gently dipping foliation of the metamorphic rocks. The minimum AMS axis is parallel to poles of foliation and dyke margins, and the fabric can be interpreted as reflecting a sub-vertical flattening (sites 32, 35, Figs. 4, 8c). This is supported with the observation at site 32, where foliation with crystal-plastic deformation is present at the dyke boundaries, but fades out inward corroborating such flattening. The maximum AMS axis plunges gently toward ESE and is parallel to one set of brittle-plastic lineations found in the surrounding metamorphic rocks (Fig. 8c), whereas the other set of metamorphic lineations has the same trend but is plunging collinearly to WNW (Fig. 8c). Although we did not observe lineation in the dyke itself, we suggest that the AMS in the dyke reflects the same deformation as observed in host metamorphic rocks. While host rocks were already cooled below 250 °C in the Oligocene (Fodor et al. 2008), we suggest that they were probably reheated in close proximity to the dykes and deformed in a transitional plastic–brittle regime together with dyke material. The other dyke in this set, located near the western tip of the intrusion, shows a penetrative foliation and a WNW plunging stretching lineation (site 35, Figs. 4, 5b, 8c). This plastic deformation pattern matches perfectly the AMS pattern, while minimum and maximum AMS axes are parallel to foliation pole and stretching lineation, respectively. The exceptionally high anisotropy of the dyke (Fig. 2) correlates with the strongly foliated texture seen both in meso- and microscale.

Within andesite and dacite dykes along the northern pluton margin, the orientation of magnetic foliations and lineations is close to that of the dyke margins and to the solid-state foliation. It is suggested therefore that the AMS reflects the crystal-plastic deformation of these dykes (Figs. 4, 5a, c, d, 8d). The AMS value is the highest when the foliation and shearing is the strongest (Fig. 2, site 51a, Fig. 5a).

All these observations show that dyke orientation and position played a crucial role in the formation of the deformation fabric; N–S oriented dykes are less deformed, while dykes parallel to pluton margin or host rock foliation exhibit larger anisotropy, and the magnetic fabric matches the mesoscale structures.

Comparison of AMS and mesoscale fault data from sediments

Sampled syn-rift sediments from the Ribnica–Selnica trough and from the western margin of the Mura depression show a good clustering of the AMS axes. After tilt correction, the minimum K_3 axes are approximately vertical, whereas the maximum K_1 axes are between NE–SW and E–W directions (Figs. 6a, 9). This geometry demonstrates that AMS fabric is bound to the bedding planes and reflects an early deformation episode before the tectonic tilting of the sediments. The only exception is site 49; K_{min} departs from the vertical considerably after tilt correction, indicating that the AMS fabric is of post-tilting age. For the youngest sediments of Middle Miocene (Badenian) age, situated northeast of the Pohorje Mts., the AMS fabric is of a compaction origin; the scattered K_1 and K_2 axes indicate the lack of detectable deformation (Fig. 6a, site 44).

Because AMS fabric mostly registers early deformation, which occurred while the beds were in a sub-horizontal position, we compared AMS data to D1(b) brittle structures which were similarly formed at the early stage of macroscopic deformation history. The D1(b) stress axes show a good match with maximum AMS axes (Figs. 6, 9), particularly at sites 40, 41 and 49. At site 48, two faulting episodes

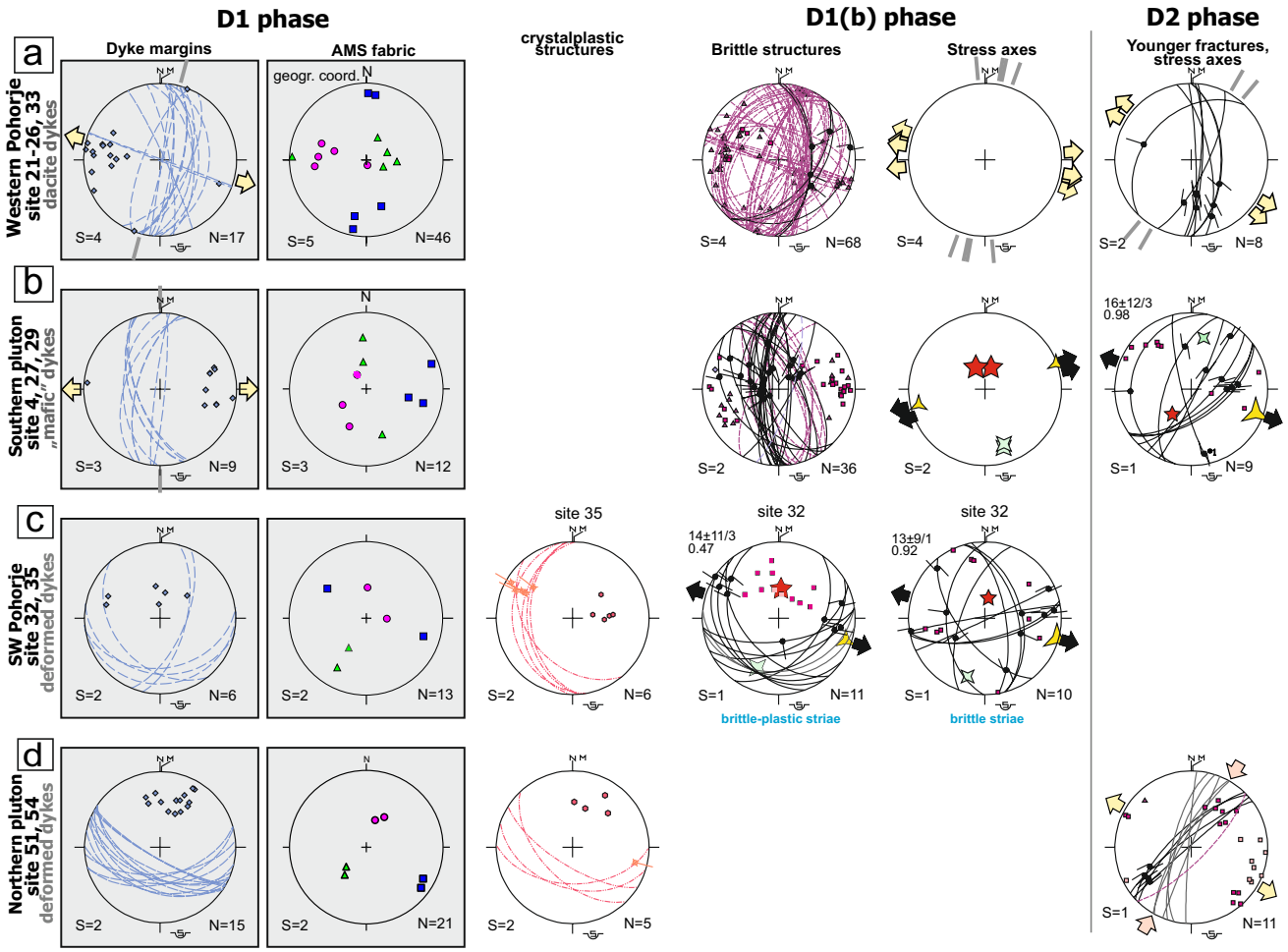

Fig. 8 Comparison of AMS and outcrop-scale structural data from dacites and mafic dykes. Legend as for Fig. 7

occurred before the tilt, and the AMS K_1 axis is between the two reconstructed σ_3 directions (Fig. 9d). Taking all these data into account, we conclude that the AMS fabric has a tectonic origin, and is not related to sediment transport. We also suggest the same tectonic origin for AMS data in sites 42–43 (Fig. 6a), although the faults recorded in the nearby site 67 do not reflect extensional but strike-slip deformation with different extension direction (Fig. 9e). For the youngest Middle Miocene (Badenian) site 44, the compactional AMS fabric is not compatible with the stress field.

SW from the Pohorje, in the Slovenj Gradec Basin, the AMS fabric of syn-rift sediments shows a very regular picture, a pre-tilt deformation with E–W stretching and vertical flattening (Fig. 6a). The paleostress inversion of fault-slip data from nearby sites S37–38 does not reflect this deformation; the calculated N–S compression can be attributed to the post-extensional D3 phase (Fig. 6b). In fact, the sampled rocks are folded, reflecting the reverse reactivation of the Periadriatic fault zone during the Pliocene–Quaternary (Fodor et al. 1998), which hampered the observation of the earliest fractures.

The direction of K_1 in the Slovenj Gradec Basin is similar to K_1 direction obtained in some sites within the Pohorje pluton, but differs from the direction characteristic for the northern Pohorje sediments. This can be due to (1) spatial variation in coeval extensional direction, (2) slight difference in age of the sediment (and the consequent difference in deformation history) or (3) differential vertical-axis rotation well after early brittle deformation and magnetic fabric formation. Similar declination–inclination data of Fodor et al. (1998) and Márton et al. (2002) both from the Pohorje sediments and Slovenj Gradec Basin (sites 40–43 and 45–47, Fig. 6) do not support this latter interpretation. New biostratigraphic data of Ivančič et al. (2018) suggest that the sediments in the Slovenj Gradec Basin are mostly Badenian, somewhat younger than the postulated Karpatian age of the northern Pohorje Mts.; this would favor scenario 2, but we cannot exclude explanation 1.

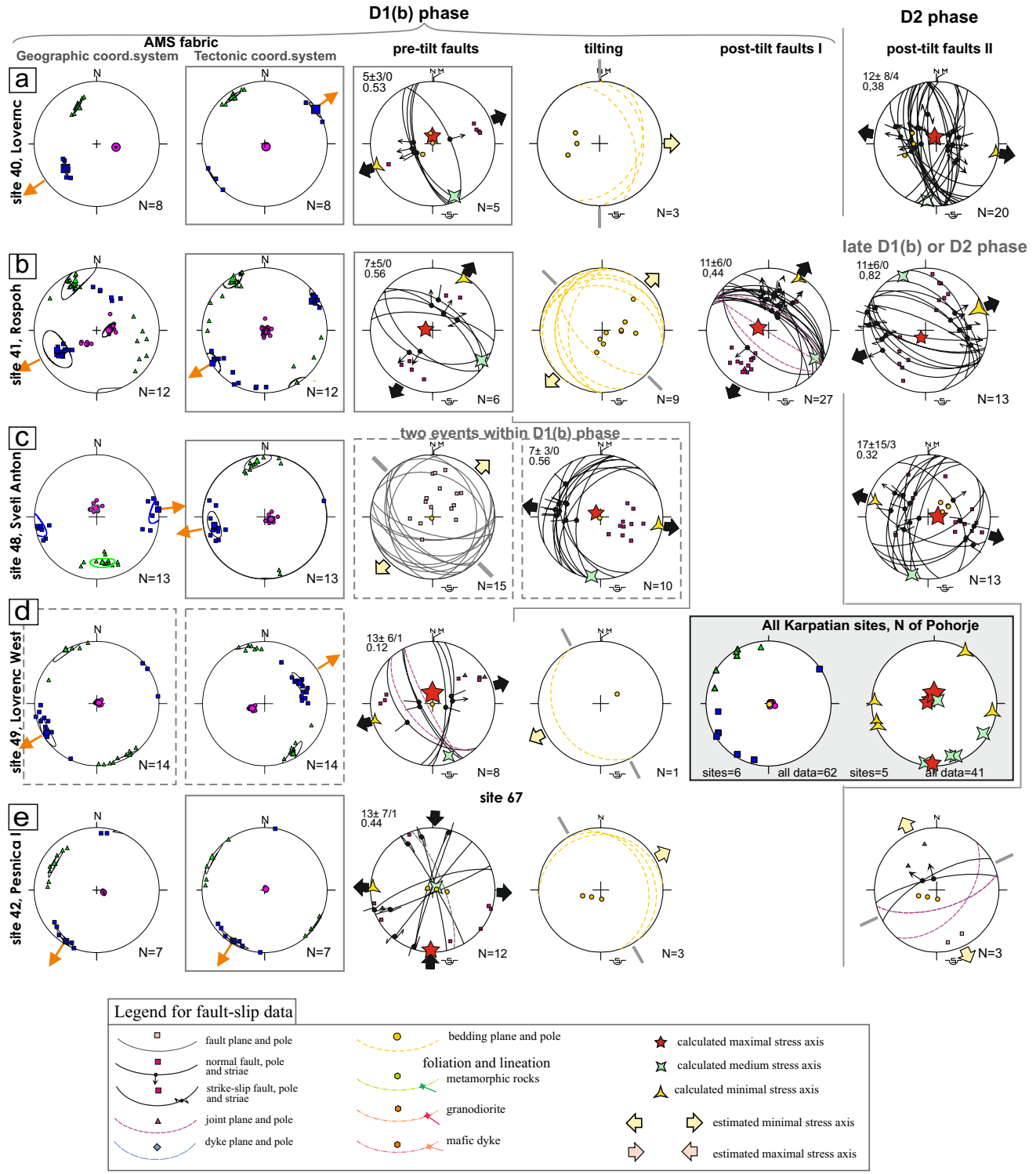

Fig. 9 Comparison of AMS and outcrop-scale structural data from Karpatian sediments in the Ribnica–Selnica trough and western Mura Basin. Legend as for Fig. 7

AMS data from metamorphic rocks

The magnetic fabric at site 34 was oriented similarly to that measured at the deformed dyke 35 which lies in close proximity (Fig. 4a). The amphibolite of site 36 has a lineation, which is close to magnetic lineation of a deformed dyke (site 32, Fig. 4a). In the southeastern Pohorje Mts. in site 37, only an inclined magnetic foliation plane was recognized. At locality 38, a large outcrop with two sets of macroscopically observable foliation planes, 15 samples from five sites were drilled. The sites comprising 38a yielded consistent AMS directions, with near-horizontal foliation planes and E–W directed lineations, while those belonging to 38b did not yield consistent results (Table 2). The near-horizontal magnetic foliation planes and E–W directed lineations are parallel to mesoscopic structural orientations and are also close to the magnetic fabric of the plutonic rocks (Fig. 4a).

All these sites show that the magnetic fabric of the metamorphic rocks is similar to that of the magmatic rocks, the sampling sites partly being situated in close vicinity of each other. This coincidence can support the Miocene origin of magnetic fabric even in the metamorphic rocks. However, their magnetic fabric could also be acquired earlier during Cretaceous shortening and extensional episodes, which exhibit tectonic transport directions similar to Miocene extension (Fodor et al. 2008).

Discussion

Magnetic properties and deformation

The comparison of anisotropy of magnetic susceptibility and mesoscale structural elements generally yields a good correlation. In most cases, the AMS axes are identical or similar in orientation to the kinematic or stress axes deduced from ductile or brittle structures. Exceptions do exist in the westernmost part of the pluton where magnetic and mineral foliations seem to be different. Thus, we infer that the AMS fabric reflects deformation of the magmatic and sedimentary rocks and is not related to other effect (e.g., intrusion, deposition, water flow).

It is thus worth comparing structural elements and other properties of the AMS. In sites where the degree of anisotropy is low (Fig. 2), we did not observe ductile deformation. This is the case in young dacite dykes and in the quartz monzodiorite body. The latter rock offers an important observation regarding the rheology of the deforming rocks and the physical conditions under which this occurred; while the quartz monzodiorite bodies are not internally deformed, the surrounding granodiorite and also their contacts with host granodiorite show intense ductile deformation (Fig. 5f). This is perfectly reflected in the AMS fabrics, with the degree of anisotropy being low in the internally undeformed quartz monzodiorite and high in the deformed granodiorite, respectively. Thus, the AMS fabric reflects the contrasting rheology of the two rock types after the incorporation of the monzodioritic blocks into the granodiorite.

The degree of anisotropy also follows the mesoscopic deformation of the dykes. The mesoscopically weakly deformed, moderately south dipping dykes (site 32) show a much lower anisotropy than the dykes with a moderate foliation (Fig. 2, sites 54, 35). At site 51a-c, we could observe changes within a few meters; dyke portions with low susceptibility show almost non-deformed magmatic texture, while the highest anisotropy was measured in sheared (mylonitic) dacite dyke (sub-sites 51a-c in Figs. 2, 5a, c, d). These observations show a strong concentration of deformation along a few selected dykes.

Inferences about the pluton geometry and emplacement

The mesoscale and microscale observations are not sufficient to clearly separate the magmatic and solid-state deformation fabrics in the plutonic rocks of the Pohorje. That is, the data do not show a clear difference in fabric orientation of the magmatic and later, solid-sate structures. Thus, we consider that the AMS reflects the combined effect of magmatic and solid-state deformation. Because the degree of anisotropy in granitoids is generally only a few percent (e.g., Hrouda and Chlupáčová 1980; Cañón-Tapia 2011; Lesić et al. 2013), we suggest that our AMS data which show a high anisotropy in the granitoids of the study area, mainly record the solid-state deformation.

Because of the lack of clear separation of magmatic and solid-state deformation texture, a characterization of the structural style of the emplacement was not possible from our data sets. The AMS fabric of the southern part of the pluton is similar to the foliation–lineation geometry of other plutons associated with extensional tectonics (Talbot et al. 2004). However, the strong solid-state deformation overprint makes such similarities of the AMS to other extensional plutons only apparent, and it is not enough to confirm an extensional origin for the Pohorje body. Nevertheless, emplacement in an extensional setting would be logical from both the regional and structural context, since the study area is located at the western margin of the crustal extension domain of the incipient Pannonian Basin, and the timing of the intrusion matches with the onset of extension. Generation of the AMS fabric occurred very soon after the emplacement, with less than 3 Ma time span between emplacement and solid-state deformation in the southern parts of the intrusion. Therefore, had the deformation style changed before the solid-state deformation started, this

change would have to have happened within this narrow time bracket.

Our combined data sets characterize well the present-day pluton geometry, after the intrusion underwent considerable solid-state deformation. Both data sets indicate vertical flattening and ~ E–W extension along the southern part of the pluton which dips below the metamorphic rocks. In the eastern part of the pluton, the lower pluton contact is exposed, as shown by our data and by earlier mapping (Kirst et al. 2010). Here, the foliation is gently dipping, but the lineation trends close to N–S, an observation that cannot be explained in our model. Moving from the east to west along the northern pluton margin, the metamorphic rocks dip below the pluton. Deformed dykes also show this geometry. The AMS and mesoscale fabrics in the north show differences when compared with the southern margin; in the north, the lineation is sub-horizontal but foliation is steep. These observations, combined with sinistral shear criteria, indicate that the deformation regime along the northern intrusion margin had a more transtensional character than in the southern one. Because the steep lateral or lower northern pluton boundary is now at the same topographic height as the southern (upper) margin, it is apparent that the whole body has been deformed on a large scale, by tilting or folding during which the northern side moved up.

Deformation and magmatic events

Micro- and mesoscale observations demonstrate that the whole Pohorje pluton as well as some related andesitic and dacitic dykes underwent solid-state deformation in the upper greenschist facies during the cooling of the pluton. Magnetic and stretching lineation indicate variable deformation orientation although a broadly E–W extension associated with sub-vertical flattening is dominant in the south and a more strike-slip type deformation occurred in the north (Fig. 4a). The dominant deformation style indicates that cooling was connected to extensional or transtensional tectonic exhumation and did not occur in a tectonically passive setting.

K–Ar ages of different mineral separates constrain dyke emplacement although ages sometimes overlap within analytical error (Fig. 1). Deformed, moderately dipping dykes intruded between 18.5 and 18.2 Ma (with uncertainties of ± 0.7 Ma), while N–S trending dykes seem to be slightly younger, ~ 17.7–17.5 Ma for mafic and 16.7–14.9 for dacite dykes (Fodor et al. 2008). The old dykes show deformation in both their AMS fabric and their meso- and microscale structures and fabrics. The younger, steeply dipping, N–trending mafic dykes show only ductile deformation in their AMS but not on a mesoscale, while the youngest dacite dykes record only magmatic flow fabric formed during emplacement. This suggests that dyke emplacement occurred during progressive cooling, and that crystal-plastic deformation gradually ceased as the regional temperature decreased. Such deformation could continue only in a limited manner, mainly near the dykes, if dyke intrusion elevated very locally the temperature above the brittle-plastic temperature threshold. Near the northern contact of the pluton, concentrated deformation and shear heating might also have contributed to maintaining crystal-plasticity.

AMS and brittle faulting in sediments

It is clear that the outcrop-scale fault patterns and the AMS fabric reflect different aspects of the deformation in the studied syn-rift sediments. The AMS depicts grain-scale features, whereas the faults are mesoscale elements. It follows that the deformation mechanisms were different on these two scales. It is suggested that the AMS fabric may characterize the earliest deformation episode, when grain rotation was still possible before it was inhibited by early diagenetic processes. Faulting might have occurred after this episode, when the sediments had acquired a certain degree of cohesion (cementation) such that trans- and intergranular fracturing could occur. However, the observed association of faulting and pronounced fault-related folding may suggest that mesoscale deformation preceded advanced cementation.

The differences between the states of deformation indicated by these two data sets may suggest that the deformations occurred at two slightly separate times. However, the similarity of AMS and stress axes orientations suggests that the two data sets reflect the same extensional deformation phase around the Pohorje pluton. Similar conclusion have been obtained from studies in other parts of the Pannonian Basin where the AMS and fault-slip data both indicate mesoscopically brittle deformation (Márton et al. 2012; Sipos-Benkő et al. 2014; Sipos et al. 2018).

In line with our conclusions, a few previous studies also suggested that the AMS textures indicate extensional deformation of the sediments. Cifelli et al. (2004, 2005) observed a maximum AMS axis perpendicular to the basin-bounding normal faults. Borradaile and Hamilton (2004) also found K_{max} perpendicular to rift margins in Cyprus. Our findings are similar to conclusions from these investigations and affirm the usefulness of AMS in sediments for unraveling early deformation episodes (Mattei et al. 1999; Cifelli et al. 2004, 2005; Márton et al. 2012).

Deformation history

The structural evolution of the pluton and surrounding sediments is shown in Fig. 10. This model extends our understanding obtained from earlier studies (Fodor et al. 2002, 2008) and emphasizes the deformation stages revealed in

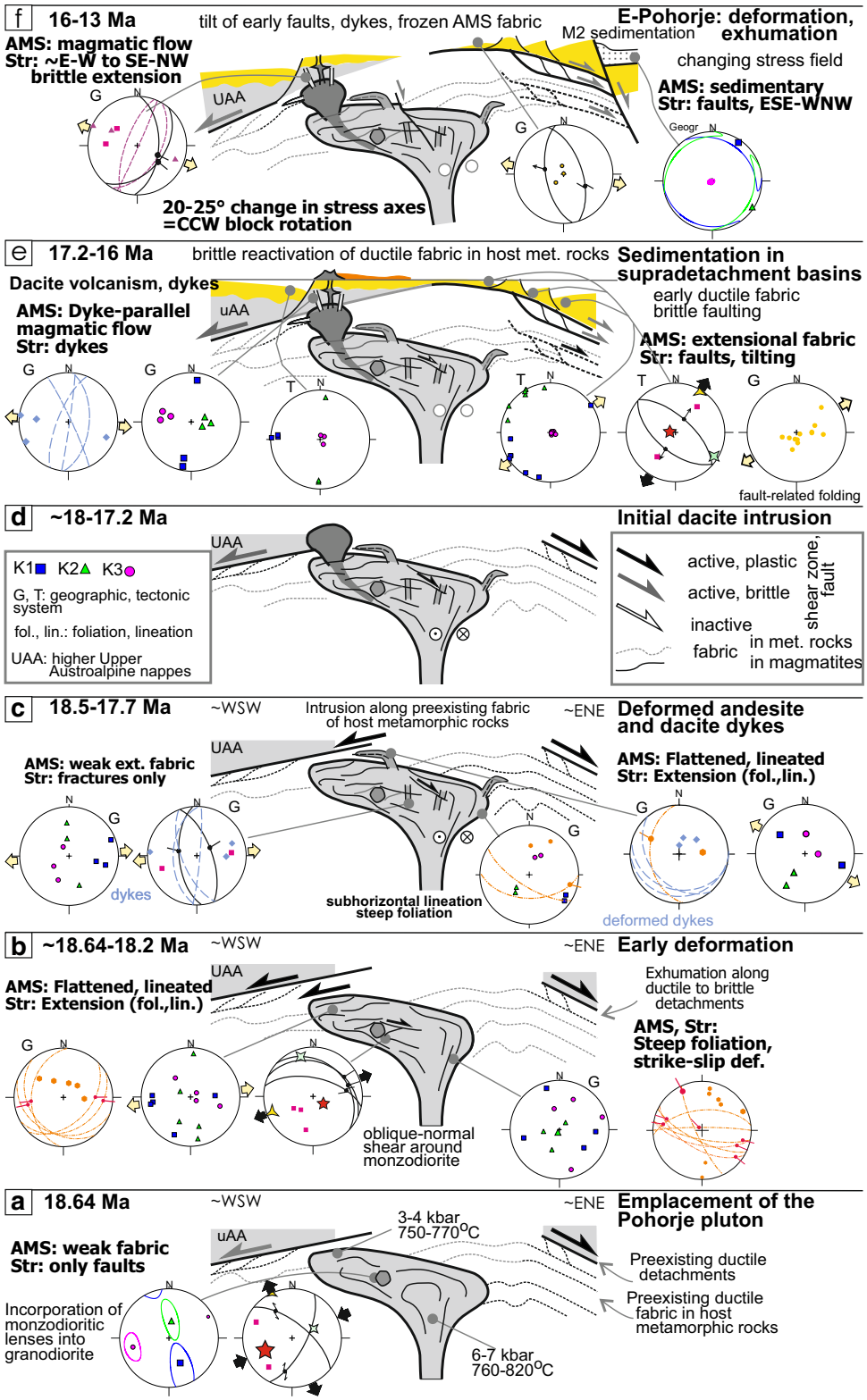

Fig. 10 Evolutionary scheme of the Pohorje pluton, modified after Fodor et al. (2008), and completed with AMS and structural data (Str). Stereograms reflect AMS data (axes only) and simplified stereograms (few characteristic faults, stress axes)

this work by the combined AMS and structural data. The intrusion of the pluton occurred at 18.64 Ma ago, and the emplacement was associated with the development of early magmatic structures; the formation of an incipient foliation and occasionally mineral lineation (Fig. 10a). It was probably during emplacement that the small quartz monzodiorite

body underwent minor internal deformation and acquired a poorly defined magnetic foliation; this deformation was followed by brittle faulting in this rock type (Fig. 10a).

Although structures could be formed at variable times on the cooling path, crystal-plastic deformation was dominant during the high-T greenschist facies conditions. This deformation predated the cooling of white mica, and K–Ar ages constrain this time span as ~ 18.5 to 16 Ma (Fodor et al. 2008; Trajanova et al. 2008). During this deformation event the dominant AMS fabric and mesoscopic foliation and lineation were formed (Fig. 10b–d). The AMS and mineral fabrics both show variable geometry in different parts of the pluton. Variable foliation/lineation patterns probably reflect the spatial heterogeneity of deformation. However, the presence of two, temporally closely spaced but distinct deformation events cannot be excluded.

Andesitic, aplitic and pegmatite dykes intruded into the pluton and host rocks between ~ 18.5 and 17.5 Ma. The strike of the steep dykes suggests ~ E–W extensional deformation during dyke emplacement. Some dykes followed preexisting ductile fabric of the host rocks, both along the gently and steeply dipping foliation planes (in the SW and NE parts of the intrusion, respectively; Fig. 10c). In the SW, dykes intruded rocks which had already been cooled to below 250–300 °C (Fodor et al. 2008). However, it is suggested that dyke intrusion could warm the adjacent country rock, and that both underwent crystal-plastic deformation, which resulted in the formation of a foliation and occasionally a lineation within these deformed, early dykes (Fig. 10c). In the northern pluton, considerable strain was accumulated in some dykes which dip moderately below the pluton. Since these deformed dykes are always less deformed than the host granodiorite, it is concluded that their emplacement postdates the early deformation of the pluton (Fig. 10b, c).

Subvolcanic dacite magmatism may have started at ~ 18 Ma (Fig. 10d). The onset of sedimentation above and around the pluton started at ~ 17.2 Ma, although the lowest sediment package could be somewhat older, ~ 19?–17.2 Ma. Fodor et al. (2002, 2008) suggest that these basins were formed above shear zones partly composed of mylonites. Low-angle detachment zones could reactivate earlier metamorphic foliations of the medium-grade rocks (Fig. 10e). During this deformation advective heat transfer affected the sediments and resulted in high vitrinite values (Sachsenhofer et al. 1998). The AMS records the earliest deformation episode which occurred, while the beds were still horizontal. Broadly, NE–SW and E–W extension was detected NE and SW of the pluton, in the Mura and Slovenj Gradec basins. It is not yet clear whether these different directions represent spatial variations in deformation, or slightly different deformation events. While still in their sub-horizontal orientation, the sediments were dissected by normal faults. They were then tilted and faulted again in a coaxial way (Fig. 10e). All these deformation events occurred before the late Badenian, ~ 14 Ma, since the sediments of this age are only weakly deformed. In the Slovenj Gradec basin the pre-tilt E-W extension was overprinted by D3 neotectonic folding.

Dacite magmatism may have started somewhat before, and was continuously active during syn-rift sedimentation (~ 17.2–15 Ma), witnessed by intercalated tuff layers and small dacite intrusions within the sediments (Fig. 10d, e). The AMS only indicates dyke-parallel magmatic flow (Fig. 10e) which is reflected neither in the mesoscopic nor in microscopic structural data. However, dyke orientation and post-cooling brittle fractures may indicate an E–W extension during the formation and cooling of the dykes.

K–Ar ages of the Pohorje Mts. indicate a tilt event during the cooling of the pluton. The tilting has resulted in different structural levels within the original pluton now occurring at similar levels in the crust (Fig. 10f). Due to this tilting, the cooling occurred somewhat later in the eastern part of the pluton. Normal faulting continued during the Badenian (15.97–12.8 Ma) and ductile shear zones were reactivated as brittle faults (Fodor et al. 2008). This deformation was not registered by the AMS data; plutonic and subvolcanic rocks were cooled and early syn-rift sediments cemented. Thus, in the youngest studied sediments, the AMS shows only sedimentary fabrics (Fig. 10f).

Faults of this phase were observed in all rock types (e.g., pluton, cooled dykes, dacite bodies, sediments). Oblique reactivation of originally dip-slip faults demonstrates a younger relative chronology for this event. Fault-slip data may indicate a slight clockwise change in the stress direction from an E–W to a SE–NW extension (Fig. 10f, from phase D1 to D2), although the data are somewhat scattered. This clockwise rotation of the stress axes would correspond to a counterclockwise block rotation of ~ 20–25°. In fact, Márton et al. (2002) observed a 45° CCW rotation in the early syn-rift sediments; thus, part of this rotation can correspond to the suggested clockwise rotation of the stress field. Further to the east, in the Pannonian Basin, CCW rotation occurred in the time span of ~ 16–15 Ma (Márton and Pécskay 1998). The amount of rotation increased from west to east, and thus was smaller in the western Pannonian Basin and in the Eastern Alps (Márton et al. 1990; Márton and Fodor 2003). The postulated Mid-Miocene rotation and subsequent apparent change in stress field in the Pohorje region is compatible with this model.

Connection with the Pannonian Basin and Eastern Alps

The time span of dominantly extensional deformation of the Pohorje rocks exactly matches the main rifting phase of the Pannonian Basin, established by combined stratigraphic and structural data sets (Tari 1994; Fodor et al. 1999; Horváth

et al. 2015). Thus, our extended and refined structural data verify the idea of Fodor et al. (2003, 2008) that the deformation and exhumation of the Pohorje pluton and the host metamorphic rocks are connected to the Pannonian rifting, which started at ~ 19 Ma (Fodor et al. 1999).

The reconstructed broadly E–W extensional direction is not very much different from other parts of the Pannonian Basin, deduced from surface stress data (Fodor et al. 1999) and subsurface fault mapping (Tari 1996); any differences can be accounted for by differential vertical-axis rotation. The deformation of the Pohorje pluton represents a deeper crustal segment having been subjected to extension. E–W to NE–SW stretching is compatible with the Miocene extensional exhumation of the Eastern Alpine deeper nappes, as demonstrated by a number of authors (Genser and Neubauer 1989; Cao et al. 2013; Schmid et al. 2013) and also with the brittle extension of the highest nappes (e.g., Frisch et al. 2000; Gruber et al. 2004; Pischinger et al. 2008). The Pohorje magmatic rocks record a stage of exhumation which is younger than the onset of this process in the Tauern window (Fig. 1), which started as early as 23 Ma (Sharf et al. 2013). On the other hand, extensional exhumation of the Pohorje rocks is coeval with the fastest exhumation period in the Tauern and the Rechnitz windows (Bertrand et al. 2017; Dunkl and Demény 1997). The extensional structures and overlying detachment zones suggest that the Pohorje intrusions represent the footwall of a basin-margin detachment zone. In this way, these rocks are part of the extensional domains surrounding the western and southern periphery of the Pannonian Basin, from the Rechnitz windows through the Medvednica (van Gelder et al. 2016) to the Moslavačka, Bukulja, Cer and Fruska Gora massifs (Ustaszewski et al. 2010; Maţenco and Radivojević 2012; Toljić et al. 2013).

Conclusions

The combined AMS and structural data set point to a dominantly extensional deformation of the Pohorje rocks although locally a transtensional setting can occur. They confirm major tectonic exhumation by extension, although the role of erosional denudation cannot be denied. All these events are thought to have happened in a relatively short time span, mainly during the magmatism, from 18.6 to 15 Ma.

The magnetic fabrics show a good correlation with the meso- and microscale deformation features. The degree of anisotropy is in agreement with macroscopic observations on strain intensity, particularly in the dykes. The strain localization is partly connected to rheological differences due to rock composition (e.g., monzodioritic blocks were not plastically deformed within granodiorite), but it is also linked to the position of the sampled rock within the magmatic complex. The shallower, dacite dykes do not show ductile deformation, and their AMS fabric is the result of magmatic flow. At shallow depths, crystal-plastic deformation was only possible very locally, around dykes, as a result of a transient increase in temperature. Although situated above the magmatic suite, the syn-rift sediments show a consistent AMS fabric, which mimics the brittle deformation observed on both outcrop- and map scale. It is thought that the magnetic fabric was acquired early in the deformation history, when the layers were horizontal and probably not completely cemented. All rock types show consecutive deformation in the same regime after cooling and cementation, while a change in stress field appears to have occurred related to vertical-axis rotation at around 15 Ma. The deformation of the Pohorje rocks is related to the formation of the Pannonian Basin and marks its western extensional margin.

Acknowledgements Open access funding provided by Eötvös Loránd University (ELTE). The major parts of the results were achieved through bilateral scientific cooperation between Slovenian and Hungarian government during the years of 1998–2003 and from funding of the Slovenian Research Agency (research core funding No. P1-0025 and P1-0195). Field work and structural analyses were also supported by the Geological Institute of Hungary. The finalization of the interpretation was supported by Hungarian research grant OTKA K83150 for László Fodor and NKFIH K128625 for Emő Márton. More recent field works were supported by a Central European Exchange Program for University Studies (CEEPUS) scholarship for Fodor, and the Hungarian research grants National Research Development and Innovation Office (NKFIH) OTKA K105245, and K113013 of Márton and Fodor, respectively. The two reviewers, John Cosgrove and Jack Nolan, contributed with many constructive remarks which improved both the scientific content and the grammar of the manuscript. The editorial help of Pavla Štípská is also acknowledged.

References

Altherr R, Lugović B, Meyer HP, Majer V (1995) Early Miocene post-collisional calc-alkaline magmatism along the easternmost segment of the Periadriatic fault system (Slovenia and Croatia). Miner Petrol 54:225–247

Angelier J (1984) Tectonic analysis of fault slip data sets. J Geophys Res 89:5835–5848

Angelier J, Manoussis S (1980) Classification automatique et distinction des phases superposée en tectonique de failles. C R Acad Sci Paris 290:651–654

Bertrand A, Rosenberg CL, Rabaute A, Herman F, Fügenschuh B (2017) Exhumation mechanisms of the Tauern Window (Eastern Alps) inferred from apatite and zircon fission track thermochronology. Tectonics. https://doi.org/10.1002/2016TC004133

Bordás R (1990) Aniso—anisotropy program package for IBM PC. Eötvös L Geophys Institute, Budapest

Borradaile GJ (1991) Correlation of strain with anisotropy of magnetic susceptibility (AMS). Pure Appl Geophys 135:15–29

Borradaile GJ, Alford C (1987) Relationship between magnetic susceptibility and strain in laboratory and experiments. Tectonophysics 133:121–135

Borradaile GJ, Hamilton T (2004) Magnetic fabrics may proxy as neotectonic stress trajectories, Polis rift, Cyprus. Tectonics 23(1):TC1001. https://doi.org/10.1029/2002TC001434

Borradaile GJ, Henry B (1997) Tectonic applications of magnetic susceptibility and its anisotropy. Earth Sci Rev 42:49–93

Borradaile GJ, Jackson M (2004) Anisotropy of magnetic susceptibility (AMS): magnetic petrofabrics of deformed rocks. In: Martín-Hernández F, Lüneburg CM, Aubourg C, Jackson, M (eds) Magnetic fabric: methods and applications. Geological Society, London, Special Publication, vol 238, pp 299–360

Bouchez JL (1997) Granite is never isotropic: an introduction to AMS studies of granitic rocks. In: Bouchez JL, Hutton DHW, Stephens WE (eds) Granite: from segregation of melt to emplacement fabrics. Petrology and structural geology, vol 8. Kluwer Publishing Co., Dordrecht, pp 95–112

Bouchez JL, Gleizes G (1995) Two-stage deformation of the Mont-Louis-Andorra granite pluton (Variscan Pyrenees) inferred from magnetic susceptibility anisotropy. J Geol Soc Lond 152:669–679

Cañón-Tapia E (2011) AMS in granites and lava flows: two end members of a continuum? In: Petrovsky E, Herrero-Bervera E, Harinarayana T, Ivers D (eds) The Earth's magnetic interior, IAGA Special Sopron Book Series 1. Springer, Dordrecht, pp 263–280

Cao S, Neubauer F, Bernroider M, Liu J, Genser J (2013) Structures, microfabrics and textures of the Cordilleran-type Rechnitz metamorphic core complex, Eastern Alps. Tectonophysics 608:1201–1225

Chadima M (2018) Anisoft 5.1.—advanced treatment of magnetic anisotropy data. Geophys Res Abstracts 20, EGU-2018-15017

Chadima M, Jelínek V (2008) Anisoft 4.2.—anisotropy data browser. Contrib Geophys Geodesy 38:41

Cifelli F, Mattei M, Hirt AM, Günther A (2004) The origin of tectonic fabrics in ''undeformed'' clays: the early stages of deformation in extensional sedimentary basins. Geophys Res Lett. https://doi.org/10.1029/2004GL019609

Cifelli F, Mattei M, Chadima M, Hirt AM, Hansen A (2005) The origin of tectonic lineation in extensional basins: combined neutron texture and magnetic analyses on "undeformed" clays. Earth Planet Sci Lett 235:62–78

Cifelli F, Mattei M, Chadima M, Lenser S, Hirt AM (2009) The magnetic fabric in "undeformed clays": AMS and neutron texture analyses from the Rif Chain (Morocco). Tectonophysics 466:79–88. https://doi.org/10.1016/j.tecto.2008.08.008

Djouadi MT, Gleizes G, Ferré E, Bouchez JL, Caby R, Lesquer A (1997) Oblique magmatic structures of two epizonal plutons, Hoggar, Algeria: late-orogenic emplacement in a transcurrent orogen. Tectonophysics 279:351–374

Dolar-Mantuani L (1935) Das Verhältnis der Aplite zu den Tonaliten im Massiv des Pohorje (Bächer gebirges). Geoloski Anali Balkanskog Poluostrova 12:1–165

Dunkl I, Demény A (1997) Exhumation of the Rechnitz Window at the border of Eastern Alps and Pannonian basin during Neogene extension. Tectonophysics 272:197–211

Exner C (1976) Die geologische Position der Magmatite des periadriatischen Lineaments. Verhandlungen der Geol Bundesanstalt 2:3–64

Faninger E (1970) Pohorski tonalit in njegovi diferenciati. Geologija 13:35–104

Ferré E, Teyssier C, Jackson M, Thill JW, Rainey ESG (2003) Magnetic susceptibility anisotropy: a new petrofabric tool in migmatites. J Geophys Res 108:2086. https://doi.org/10.1029/2002JB001790

Ferré EC, Gébelin A, Till JL, Sassier C, Burmeister CK (2014) Deformation and magnetic fabrics in ductile shear zones: a review. Tectonophysics 629:179–188

Fodor L, Jelen B, Márton E, Skaberne D, Čar J, Vrabec M (1998) Miocene-Pliocene tectonic evolution of the Slovenian Periadriatic fault: implication for Alpine-Carpathian extrusion models. Tectonics 17:690–709

Fodor L, Csontos L, Bada G, Györfi I, Benkovics L (1999) Tertiary tectonic evolution of the Pannonian basin system and neighbouring orogens: a new synthesis of paleostress data. In: Durand B, Jolivet L, Horváth F, Séranne M (eds) The Mediterranean basins: Tertiary extension within the Alpine Orogen. Geological Society, London, Special Publication, vol 156, pp 295–334

Fodor L, Jelen B, Márton E, Rifelj H, Kraljić M, Kevrić R, Márton P, Koroknai B, Báldi-Beke M (2002) Miocene to Quaternary deformation, stratigraphy and paleogeography in Northeastern Slovenia and Southwestern Hungary. Geologija 45:103–114

Fodor L, Balogh K, Dunkl I, Pécskay Z, Koroknai B, Trajanova M, Vrabec M, Vrabec M, Horváth P, Janák M, Lupták B, Frisch W, Jelen B, Rifelj H (2003) Structural evolution and exhumation of the Pohorje-Kozjak Mts., Slovenia. Annales Universitatis Scientiarum Budapestiensis de R Eötvös Nominatae 35:118–119

Fodor L, Gerdes A, Dunkl I, Koroknai B, Pécskay Z, Trajanova M, Horváth P, Vrabec M, Jelen B, Balogh K, Frisch W (2008) Miocene emplacement and rapid cooling of the Pohorje pluton at the Alpine-Pannonian-Dinaric junction: a geochronological and structural study. Swiss J Earth Sci 101:255–271

Frisch W, Dunkl I, Kuhlemann J (2000) Postcollisional orogen-parallel large-scale extension in the Eastern Alps. Tectonophysics 327:239–265

Genser J, Neubauer F (1989) Low angle normal faults at the eastern margin of the Tauern Window. Mitt Österr Geol Ges 81:233–243

Georgiev N, Henry B, Jordanova N, Jordanova D, Naydenov K (2014) Emplacement and fabric-forming conditions of plutons from structural and magnetic fabric analysis: a case study of the Plana pluton (Central Bulgaria). Tectonophysics 629:138–154

Graham J. Borradaile, Tom Hamilton (2004) Magnetic fabrics may proxy as neotectonic stress trajectories, Polis rift, Cyprus. Tectonics 23(1)

Graham JW (1954) Magnetic susceptibility anisotropy, an unexploited petrofabric element. Geol Soc Am Bull 65:1257–1258

Gruber W, Sachsenhofer RF, Kofler N, Decker K (2004) The architecture of the intramontane Trofaiach pull-apart basin inferred from geophysical and structural studies. Geol Carpath 55:281–298

Harangi SZ, Mason PRD, Lukács R (2005) Correlation and petrogenesis of silicic pyroclastic rocks in the northern Pannonian Basin, Eastern central Europe: in situ trace element data of glass shards and mineral chemical constraints. J Volc Geothermal Res 143:237–257

Hinterlechner-Ravnik A (1971) The Pohorje Mountains metamorphic rocks I. Geologija 30:187–226

Hinterlechner-Ravnik A (1988) Garnet peridotite from the Pohorje Mountains. Geologija 30:149–181 (in Slovenian)

Horváth F, Musitz B, Balázs A, Végh A, Uhrin A, Nádor A, Koroknai B, Pap N, Tóth T, Wórum G (2015) Evolution of the Pannonian Basin and its geothermal resources. Geothermics 53:328–352

Hrouda F, Chlupáčová M (1980) The magnetic fabric in the Nasavrky massif. Casopis pro mineralogii a geologii 25:17–27
Hrouda F, Janák F (1976) The changes in shape of the magnetic susceptibility ellipsoid during progressive metamorphism and deformation. Tectonophysics 34:135–148
Hrouda F, Jelínek V, Hrušková L (1990) A package of programs for statistical evaluation of magnetic anisotropy data using IBM-PC computers. EOS Trans AGU Fall meeting 1990
Ivančič K, Trajanova M, Ćorić S, Rožič B, Šmuc A (2018) Miocene paleogeography and biostratigraphy of the Slovenj Gradec Basin: a marine corridor between the Mediterranean and Central Paratethys. Geol Carpath 69:528–544. https://doi.org/10.1515/geoca-2018-0031
Janák M, Froitzheim N, Lupták B, Vrabec M, Krogh Ravna EJ (2004) First evidence for ultrahighpressure metamorphism of eclogites in Pohorje, Slovenia: tracing deep continental subduction in the Eastern Alps. Tectonics 23:1–6. https://doi.org/10.1029/2004TC001641
Janák M, Froitzheim N, Yoshida K, Sasinkova V, Nosko M, Kobayashi T, Hirajima T, Vrabec M (2015) Diamond in metasedimentary crustal rocks from Pohorje, Eastern Alps: a window to deep continental subduction. J Met Geol. https://doi.org/10.1111/jmg.12130
Jelen B, Rifelj H (2003) The Karpatian in Slovenia. In: Brzobohatý R, Cicha M, Kováč M, Rögl F (eds) The Karpatian: a lower miocene stage of the Central Paratethys. Masaryk University, Brno, pp 133–139
Jelínek V (1977) The statistical theory of measuring anisotropy of magnetic susceptibility of rocks and its application. Geofyzika Brno, Czechoslovakia, p 88
Jelínek V (1978) Statistical processing of anisotropy of magnetic susceptibility measured on groups of sediments. Stud Geophys Geod 22:50–62
Jelínek V (1981) Characterization of magnetic fabric of rocks. Tectonophysics 79:T63–T67
Kieslinger A (1935) Geologie und Petrologie des Bachern. Verh der Geol Bundesanst 7:101–110
Kirst F, Sandmann S, Nagel JT, Froitzheim N, Janák M (2010) Tectonic evolution of the southeastern part of the Pohorje Mountains (Eastern Alps, Slovenia). Geol Carpath 61:451–461. https://doi.org/10.2478/V10096-010-0027-Y
Kratinová Z, Schulmann K, Edel J-B, Ježek J, Schaltegger U (2007) Model of successive granite sheet emplacement in transtensional setting: integrated microstructural and anisotropy of magnetic susceptibility study. Tectonics. https://doi.org/10.1029/2006TC002035
Lesić V, Márton E, Cvetkov V, Tomić D (2013) Magnetic anisotropy of Cenozoic igneous rocks from the Vardar zone (Kopaonik area, Serbia). Geophys J Int 193:1182–1197. https://doi.org/10.1093/gji/ggt062
Mancktelow NS, Pennacchioni G (2013) Late magmatic healed fractures in granitoids and their influence on subsequent solid-state deformation. J Struct Geol 57:81–96
Márton E, Fodor L (2003) Tertiary paleomagnetic results and structural analysis from the Transdanubian Range (Hungary); sign for rotational disintegration of the Alcapa unit. Tectonophysics 363:201–224
Márton E, Pécskay Z (1998) Correlation and dating of the Miocene ignimbritic volcanics in the Bükk foreland, Hungary: complex evaluation of paleomagnetic and K/Ar isotope data. Acta Geol Hung 41:467–476
Márton E, Fodor L, Jelen B, Márton P, Rifelj H, Kevrić R (2002) Miocene to Quaternary deformation in NE Slovenia: complex paleomagnetic and structural study. J Geodyn 34:627–651
Márton E, Trajanova M, Fodor L, Koroknai B, Vrabec M, Vrabec M, Zupancic N (2004) Magnetic fabrics of the Pohorje igneous-metamorphic complex (Slovenia) related to deformation. Contrib Geophys Geod 34:91–92
Márton E, Trajanova M, Zupančič N, Jelen B (2006) Formation, uplift and tectonic integration of a Periadriatic intrusive complex (Pohorje, Slovenia) as reflected in magnetic parameters and paleomagnetic directions. Geophys J Int 167:1148–1159
Márton E, Tomljenović B, Pavelić D, Pethe M, Jelen B (2012) Magnetic fabric of Late Miocene clayrich sediments from the southern Pannonian basin. Int J Earth Sci 101:879–888. https://doi.org/10.1007/s00531-011-0669-8
Maţenco L, Radivojević D (2012) On the formation and evolution of the Pannonian Basin: constraints derived from the structure of the junction area between the Carpathians and Dinarides. Tectonics 31:67. https://doi.org/10.1029/2012TC003206
Mattei M, Speranza F, Argentieri A, Rossetti F, Sagnotti L, Funiciello R (1999) Extensional tectonics in the Amantea basin (Calabria, Italy): a comparison between structural and magnetic anisotropy data. Tectonopysics 307:33–49
Miller C, Mundil R, Thöni M, Konzett J (2005) Refining the timing of eclogite metamorphism: a geochemical, petrological, Sm-Nd and U-Pb case study from the Pohorje Mountains, Slovenia (Eastern Alps). Contrib Miner Petrol 150:70–84
Mioč P (1977) Geologic structure of the Drava Valley between Dravograd and Selnica. Geologija 20:193–230
Mioč P, Žnidarčič M (1977) Geological map of the sheet Slovenj Gradec, L 33-55, 1:100000. Federal Geological Survey of Yugoslavia, Belgrade
Pamić J, Pálinkaš L (2000) Petrology and geochemistry of Paleogene tonalites from the easternmost parts of the Periadriatic Zone. Miner Petrol 70:121–141
Parés JM, van der Pluijm BA (2002) Evaluating magnetic lineations (AMS) in deformed rocks. Tectonophysics 350:283–298
Paterson SR, Vernon RH, Tobisch OT (1989) A review of criteria for the identification of magmatic and tectonic foliations in granitoids. J Struct Geol 11:349–363
Pécskay Z, Lexa J, Szakács A, Szegedi I, Balogh K, Konečny V, Zelenka T, Kovacs M, Póka T, Fülöp A, Márton E, Panaiotu C, Cvetković V (2006) Geochronology of Neogene magmatism in the Carpathian arc and intra-Carpathian area. Geol Carpath 57:511–530
Pischinger G, Kurz W, Übleis M, Egger M, Fritz H, Brosch FJ, Stingl K (2008) Fault slip analysis in the Koralm Massif (Eastern Alps) and consequences for the final uplift of "cold spots" in Miocene times. Swiss J Earth Sci 101:235–254
Pomella H, Klötzli U, Scholger R, Stipp M, Fügenschuh B (2011) The Northern Giudicarie and the Meran-Mauls fault (Alps, Northern Italy) in the light of new paleomagnetic and geochronological data from boudinaged Eo-/Oligocene tonalities. Int J Earth Sci 100:1827–1850. https://doi.org/10.1007/s00531-010-0612-4
Rosenberg CL (2004) Shear zones and magma ascent: a model based on a review of the Tertiary magmatism in the Alps. Tectonics. https://doi.org/10.1029/2003TC001526
Sachsenhofer RF, Dunkl I, Hasenhüttl Ch, Jelen B (1998) Miocene thermal history of the southwestern margin of the Styrian Basin: coalification and fission track data from the Pohorje/Kozjak area (Slovenia). Tectonophysics 297:17–29
Sandmann S, Herwartz D, Kirst F, Froitzheim N, Nagel TJ, Fonseca ROC, Münker C, Janák J (2016) Timing of eclogite-facies metamorphism of mafic and ultramafic rocks from the Pohorje Mountains (Eastern Alps, Slovenia) based on Lu–Hf garnet geochronometry. Lithos 262:576–585. https://doi.org/10.1016/j.lithos.2016.08.002
Sant K, Palcu DV, Mandic O, Krijgsman W (2017) Changing seas in the Early-Middle Miocene of Central Europe: a Mediterranean approach to Paratethyan stratigraphy. Terra Nova 29:273–281. https://doi.org/10.1111/ter.12273

Schmid S, Sharf A, Handy M, Rosenberg C (2013) The Tauern Window (Eastern Alps, Austria): a new tectonic map, with cross-sections and a tectonometamorphic synthesis. Swiss J Geosci 106:1–32. https://doi.org/10.1007/s00015-013-0123-y

Sharf A, Handy M, Favaro S, Schmid S, Bertrand A (2013) Modes of orogen-parallel stretching and extensional exhumation in response to microplate indentation and roll-back subduction (Tauern Window, Eastern Alps). Int J Earth Sci 102:1627–1654. https://doi.org/10.1007/s00531-013-0894-4

Sidman D, Ferré EC, Teyssier C, Jackson M (2015) Magnetic fabric and microstructure of a mylonite: example from the Bitterroot shear zone, western Montana. Geol Soc Lond Spec Publ 245:143–163. https://doi.org/10.1144/GSL.SP.2005.245.01.07

Sipos AA, Márton E, Fodor L (2018) Reconstruction of early phase deformations by integrated magnetic and mesotectonic data evaluation. Tectonophysics 726:73-85

Sipos-Benkő K, Márton E, Fodor L, Pethe M (2014) An integrated anisotropy of magnetic susceptibility and structural geological study on Cenozoic clay rich sediments from the Transdanubian Range, Hungary. Central Eur Geol 57:21–52

Sotelšek T, Jarc S, Zupančič N, Vrabec M (2019) The crystallization depth of quartz monzodiorite from Pohorje Mountains. In: Pirker L (ed) 3rd meeting of Slovenian microscopists, Ljubljana, 2019, 72, COBISS.SI-ID 1481822

Stevenson CTE, Owens WH, Hutton DHW (2007) Flow lobes in granite: the determination of magma flow direction in the Trawenagh Bay Granite, northwestern Ireland, using anisotropy of magnetic susceptibility. Geol Soc Am Bull 119:1368–1386. https://doi.org/10.1130/B25970.1

Stipp M, Stuenitz H, Heilbronner R, Schmid SM (2002) The eastern Tonale fault zone: a "natural laboratory" for crystal plastic deformation of quartz over a temperature range from 250 to 700 C. J Struct Geol 24:1861–1884

Talbot J-Y, Martelet G, Courrioux G, Chen Y, Faure M (2004) Emplacement in an extensional setting of the Mont Lozère-Borne granitic complex (SE France) inferred from comprehensive AMS, structural and gravity studies. J Struct Geol 26:11–28

Tari G (1994) Alpine Tectonics of the Pannonian basin. PhD Thesis, Rice University, Texas, USA

Tari G (1996) Extreme crustal extension in the Rába river extensional corridor (Austria/Hungary). Mitt Gesell Geol Bergbaustud Österreich 41:1–18

Tarling DH, Hrouda FH (1993) The magnetic anisotropy of rocks. Chapman & Hall, London

Till JL, Jackson MJ, Moskowitz BM (2010) Remanence stability and magnetic fabric development in synthetic shear zones deformed at 500°C. Geochem Geophys Geosyst. https://doi.org/10.1029/2010GC003320

Toljić M, Maţenco L, Ducea MN, Stojadinović U, Milivojević J, Đerić N (2013) The evolution of a key segment in the Europe-Adria collision: the Fruška Gora of northern Serbia. Glob Planet Change 103:39–62

Trajanova M (2002) Significance of mylonites and phyllonites in the Pohorje and Kobansko area. Geologija 45:149–161

Trajanova M (2013) Age of the Pohorje Mountains magmatism; new view on the origin of the Pohorje tectonic block. PhD Thesis, Ljubljana (in Slovenian)

Trajanova M, Pécskay Z, Itaya T (2008) K–Ar geochronology and petrography of the Miocene Pohorje Mountains batholith (Slovenia). Geol Carpath 59:247–260

Ustaszewski K, Kounov A, Schmid SM, Schaltegger U, Krenn E, Frank W et al (2010) Evolution of the Adria-Europe plate boundary in the northern Dinarides: from continent-continent collision to back-arc extension. Tectonics. https://doi.org/10.1029/2010tc002668

van Gelder IE, Maţenco L, Willingshofer E, Tomljenović B, Andriessen PAM, Ducea MN, Beniest A, Gruić A (2016) The tectonic evolution of a critical segment of the Dinarides-Alps connection: Kinematic and geochronological inferences from the Medvednica Mountains, NE Croatia. Tectonics 34:1952–1978. https://doi.org/10.1002/2015TC003937

Vrabec M, Janák M, Froitzheim N, De Hoog JCM (2012) Phase relations during peak metamorphism and decompression of the UHP kyanite eclogites, Pohorje Mountains (Eastern Alps, Slovenia). Lithos 144–145:40–55. https://doi.org/10.1016/j.lithos.2012.04.004

Winkler A (1929) Über das Alter der Dazite im Gebiete des Draudurchbruches. Verhandl Geol Bundesanst 8:169–181

Zhou Y, Zhou P, Wu SM, Shi XB, Zhang JJ (2002) Magnetic fabric study across the Ailao Shan-Red River shear zone. Tectonophysics 346:137–150

Žnidarčič M, Mioč P (1988) Geological map of the sheets Maribor and Leibnitz, L 33-56 and L 33-44, 1:100 000. Federal Geol Surv of Yugoslavia, Belgrade

Zupančič N (1994) Geokemične značilnosti in nastanek pohorskih magmatskih kamnin. (Geochemical characteristics and origin of the Pohorje igneous rocks). Rud-metal zb 41:113–128